5476 J. Med. Chem. 2010, 53, 5476–5490
DOI: 10.1021/jm100027p

Journal of Medicinal Chemistry Article

Quinazolin-4-one Derivatives: A Novel Class of Noncompetitive NR2C/D Subunit-Selective *N*-Methyl-D-aspartate Receptor Antagonists

Cara A. Mosley,[†] Timothy M. Acker,[†,‡] Kasper B. Hansen,[‡] Praseeda Mullasseril,[‡] Karen T. Andersen,[‡,§] Phuong Le,[‡] Kimberly M. Vellano,[‡] Hans Bräuner-Osborne,[§] Dennis C. Liotta,*[,†] and Stephen F. Traynelis*[,‡]

[†]*Department of Chemistry, Emory University, 1515 Dickey Drive, Atlanta, Georgia 30033,* [‡]*Department of Pharmacology, Emory University School of Medicine, Rollins Research Center 1510 Clifton Road, Atlanta, Georgia 30322, and* [§]*Department of Medicinal Chemistry, Faculty of Pharmaceutical Sciences, University of Copenhagen, Copenhagen, Denmark*

Received January 30, 2010

We describe a new class of subunit-selective antagonists of *N*-methyl D-aspartate (NMDA)-selective ionotropic glutamate receptors that contain the (*E*)-3-phenyl-2-styrylquinazolin-4(3*H*)-one backbone. The inhibition of recombinant NMDA receptor function induced by these quinazolin-4-one derivatives is noncompetitive and voltage-independent, suggesting that this family of compounds does not exert action on the agonist binding site of the receptor or block the channel pore. The compounds described here resemble CP-465,022 ((*S*)-3-(2-chlorophenyl)-2-[2-(6-diethylaminomethyl-pyridin-2-yl)-vinyl]-6-fluoro-3*H*-quinazolin-4-one), a noncompetitive antagonist of AMPA-selective glutamate receptors. However, modification of ring substituents resulted in analogues with greater than 100-fold selectivity for recombinant NMDA receptors over AMPA and kainate receptors. Furthermore, within this series of compounds, analogues were identified with 50-fold selectivity for recombinant NR2C/D-containing receptors over NR2A/B containing receptors. These compounds represent a new class of noncompetitive subunit-selective NMDA receptor antagonists.

Introduction

N-Methyl-D-aspartate (NMDA[a]) receptors are ligand-gated cation-selective channels that mediate glutamatergic excitatory synaptic transmission in the central nervous system.[1] A wide range of roles have been proposed for NMDA receptors, including neuronal development[2−5] and synaptic plasticity underlying learning.[6,7] In addition, aberrant activation of NMDA receptors has been suggested to participate in neuropathological conditions such as stroke, epilepsy, schizophrenia, depression, Alzheimer's disease, Huntington's disease, and Parkinson's disease.[8−15]

NMDA receptors are tetrameric assemblies of two glycine-binding NR1 subunits and two glutamate-binding NR2 subunits, of which there are four subtypes (NR2A, NR2B, NR2C, NR2D). The NR2 subunit appears to control pharmacological properties, response time course, and channel properties.[16−22] In particular, receptors containing NR2C or NR2D subunits are activated by glycine and glutamate with higher potency than receptors containing NR2A or NR2B. NMDA receptors containing NR2C or NR2D also show lower maximal open probability than receptors containing NR2A or NR2B. NR2D-containing NMDA receptors have been hypothesized to show exceptionally slow deactivation following removal of glutamate. NR2C and NR2D subunits also show localization patterns distinct from NR2A and NR2B, with prominent expression in cerebellum, discrete nuclei within the basal ganglia, and select populations of interneurons.[23−37] The distinct anatomical localization of the NR2 subunits raises the possibility that subunit-selective antagonists and allosteric modulators might provide well-tolerated therapeutic treatments for a wide range of indications.[1]

Ifenprodil was the first subunit-selective NMDA receptor antagonist identified, showing over 200-fold selectivity at NR2B over NMDA receptors containing other NR2 subunits.[38−41] Despite intense interest in NMDA receptors and their hypothesized roles in numerous neurological disorders, no antagonists that are more than 10-fold selective for NR2A, NR2C, or NR2D have yet been identified.[42−46] The inability to identify subunit-selective competitive antagonists may reflect the highly conserved glutamate-binding pocket within the NR2 subunit.[47,48] Channel blockers are similarly poorly selective for NMDA receptors comprised of different NR2 subunits,[49] presumably due to structural conservation of the permeation pore. The lack of subunit-selective pharmacological tools for this receptor class has been an impediment to understanding the functional roles of the NR2A, NR2C, and NR2D subunits in neurons. Because NMDA receptor architecture appears to reflect the assembly of multiple extracellular semiautonomous domains,[50−52] we hypothesized that the multiple protein−protein interfaces within the NMDA receptor may provide new targets for modulating NMDA receptor function. To search

*To whom correspondence should be addressed. For Chemistry (D.C.L.): phone, 404 727 6602; fax, 404 412 8649; E-mail, dliotta@emory.edu. For Biology (S.F.T.): phone, 404 727 0357; fax, 404 727 0365; E-mail, strayne@emory.edu.

[a]Abbreviations: AMPA, α-amino-3-hydroxy-5-methyl-4-isoxazolepropionic acid; BAPTA-AM, 1,2-bis(*o*-aminophenoxy)ethane-*N*,*N*,*N*′,*N*′-tetraacetic acid tetraacetoxymethyl ester; cDNA, cDNA; DMSO, dimethyl sulfoxide; HPLC, high performance liquid chromatography; IC_{50}, concentration of a test compound that produces half maximal inhibition; K-BAPTA, potassium 1,2-bis(*o*-aminophenoxy)ethane-*N*,*N*,*N*′,*N*′-tetraacetic acid; NMDA, *N*-methyl-D-aspartate; NMR, nuclear magnetic resonance.

 Published on Web 07/13/2010

for modulators that might interact at these interfaces, we executed a multiwell fluorescence-based assay to identify novel noncompetitive inhibitors of recombinant NMDA receptors.[53] Screening a diversity library of compounds with this assay allowed us to identify a new class of recombinant NMDA receptor antagonists that contains the quinazolin-4-one backbone, which is shared with the previously reported α-amino-3-hydroxy-5-methyl-4-isoxazolepropionic acid (AMPA) receptor-selective noncompetitive antagonist CP-465,022 (**1**, Figure 1).[54−56] NMDA receptor inhibition was voltage-independent and noncompetitive (Supporting Information Figure S1). Synthetic efforts toward optimizing backbone substituents led to the development of a structure−activity relationship (SAR), ultimately yielding novel compounds with between 50- and 100-fold selectivity for recombinant NR2C/D- over NR2A/B-containing receptors. The half-maximal inhibiting concentrations of members of this class are in the low micromolar range (IC_{50} = 0.6−6 μM) at recombinant NMDA receptors, with no detectable activity at recombinant kainate receptors and variable activity at recombinant AMPA receptors.

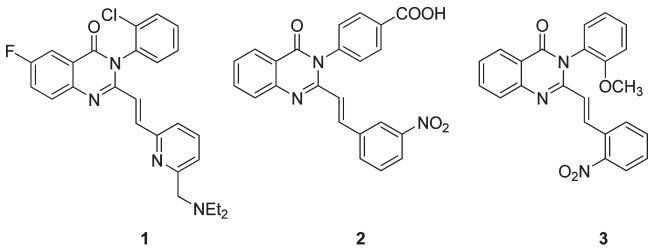

Figure 1. Structures for CP-465,022 (**1**), (*E*)-4-(2-(3-nitrostyryl)-4-oxoquinazolin-3(4*H*)-yl)benzoic acid (**2**), and (*E*)-3-(2-methoxyphenyl)-2-(2-nitrostyryl)quinazolin-4(3*H*)-one (**3**).

Results

Chemistry. We evaluated both commercially available analogues and a number of synthetic styryl quinazolin-4-one analogues that were generated via a three-step sequence which combines commercially available fragments: anthranilic acids, anilines, and aldehydes (Scheme 1). Briefly, a substituted anthranilic acid (**4**) was converted to the benzoxazin-4-one (**5**) by refluxing in acetic anhydride. The quinazolin-4-one core (**6**) was generated by a ring-opening−ring-closure reaction under acidic conditions in the presence of a substituted aniline. Finally, acid-catalyzed condensation reaction of **6** with a substituted aldehyde yielded the target (*E*)-3-phenyl-2-styrylquinazolin-4(3*H*)-one.

An alternative methodology was utilized to synthesize analogues for which the starting material anthranilic acids were not commercially available (Scheme 2). Protection of the carboxylic acid of **78** with *tert*-butyldimethylsilyl chloride

Scheme 1. Synthesis of (*E*)-3-Phenyl-2-styrylquinazolin-4(3*H*)-ones[a]

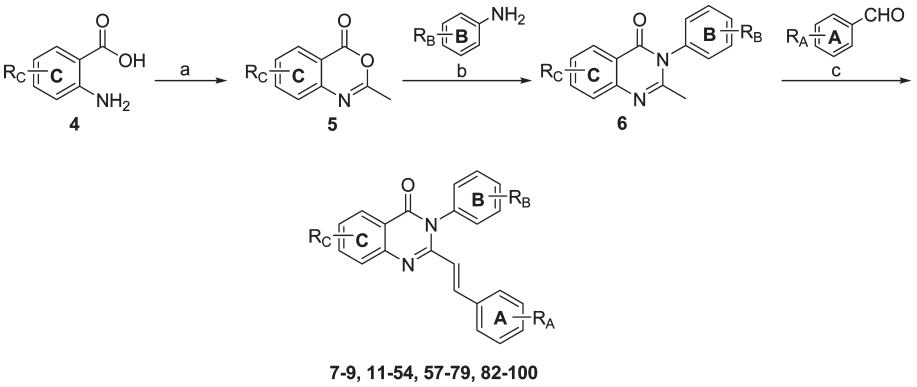

[a] (a) Ac_2O, reflux; (b) AcOH, reflux; (c) Ac_2O, AcOH, NaOAc, reflux.

Scheme 2. Suzuki Route for Synthesis of (*E*)-3-Phenyl-2-styrylquinazolin-4(3*H*)-ones[a]

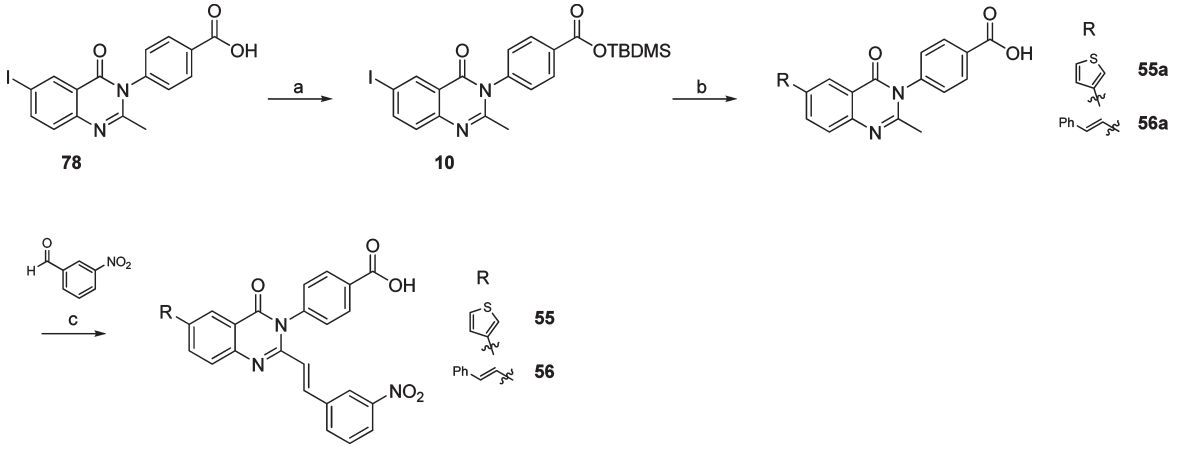

[a] (a) TBDMSCl, NMM, THF; (b) $RB(OH)_2$, $Pd(PPh_3)_4$, aq $NaHCO_3$, 1,2-DME, reflux; (c) Ac_2O, AcOH, NaOAc, reflux.

(TBDMSCl) and *N*-methylmorpholine gave **10**.[57] Suzuki coupling between **10** and the appropriately substituted boronic acid afforded C ring R_8-substituted quinazolinones **55a** and **56a**. The TBDMS protecting group was removed with the addition of 1.0 N hydrochloric acid (HCl) during workup. A condensation reaction of **55a** or **56a** with *meta*-nitrobenzaldehyde gave **55** and **56**. Reduction of the styryl linker present in **80** with hydrogenolysis yielded the fully saturated linker compound **81** (Scheme 3).

Quniazolin-4-ones Inhibit NMDA Receptors. Completion of a fluorescence-based[58] screen of 83,880 compounds from ChemDiv and Asinex libraries of small molecules on NMDA receptor responses in both NR1/NR2D and NR1/NR2C cell lines yielded a 0.16% hit rate; all hits were confirmed by two-electrode voltage-clamp recording. A number of active compounds in this assay shared a quinazolin-4-one backbone, typified by (*E*)-4-(2-(3-nitrostyryl)-4-oxoquinazolin-3(4*H*)-yl)benzoic acid (**2**) and (*E*)-3-(2-methoxyphenyl)-2-(2-nitrostyryl)quinazolin-4(3*H*)-one (**3**) (see Figure 1). Quinazolin-4-one derivatives have previously been shown to be potent and relatively selective AMPA receptor antagonists.[54−56] Compounds **2** and **3** inhibited NR1/NR2C and NR1/NR2D responses completely with fitted IC_{50} values in the micromolar range (IC_{50} values 9 and 5 μM, respectively, at NR1/NR2D). Inhibition by 30 μM of compound **2** was noncompetitive at NR1/NR2D receptors, in that it could not be surmounted by increasing the concentration of glutamate and glycine from 100/30 μM to 1000/300 μM ($n = 4$; Figure S1 in Supporting Information). Moreover, inhibition of NR1/NR2D responses by 10 μM of compound **2** was voltage-independent, with no significant difference in inhibition at −40 mV compared to +40 mV ($p > 0.05$; *t* test; $n = 5$; Figure S1 in Supporting Information). These data suggest that quinazolin-4-ones are noncompetitive antagonists of NR1/NR2D NMDA receptors that likely act at a site independent of the channel pore. Inhibition of NR1/NR2C receptors by compound **2** was similarly complete at saturating concentrations ($n = 8$), noncompetitive ($n = 6$), and voltage-independent ($n = 6$).

Positional Isomer Manipulation of Screening Hits 2 and 3. The screening hits, compounds **2** and **3**, were inactive at kainate receptors, and 4−5-fold more potent (i.e., lower fitted IC_{50}) at NMDA receptors than AMPA receptors (Table 1). Analogues lacking substitutions on all aryl rings

Scheme 3. Synthesis of **81**[a]

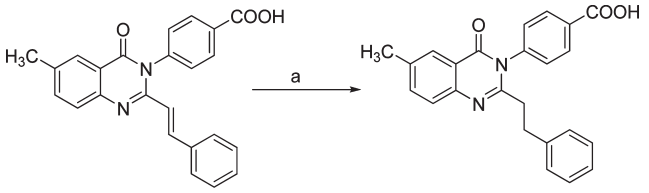

80 **81**

[a] (a) H_2, Pd/C, DMF.

Table 1. Optimization of Subunit Selectivity through Evaluation of Ring A and Ring B Substituent Positions[a]

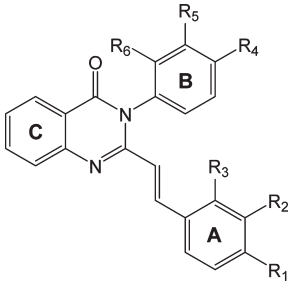

no.	R_1	R_2	R_3	R_4	R_5	R_6	NR2A IC_{50}	NR2B IC_{50}	NR2C IC_{50}	NR2D IC_{50}	GluR1 IC_{50}	GluR6 IC_{50}	NR2A[b]/NR2D	GluR1[c]/NR2D
7	NO_2			COOH			64	93	15	15	> 300	NE	4	> 20
8	NO_2				COOH		135	177	33	27	> 300	NE	5	> 10
9	NO_2					COOH	> 300	197	> 300	278	> 300	NE	1	1
2		NO_2		COOH			21	30	12	9	32	NE	2	4
11		NO_2			COOH		100	69	19	15	32	NE	7	2
12		NO_2				COOH	> 300	235	258	148	> 300	NE	2	2
13			NO_2	COOH			11	17	8	6	6	NE	2	1
14			NO_2		COOH		17	20	8	7	5	NE	2	1
15*[d]	NO_2			OCH_3			> 300	98	181	221	> 300	NE	1	1
16*[d]	NO_2				OCH_3		> 300	> 300	> 300	> 300	> 300	NE	1	1
17*[d]	NO_2					OCH_3	> 300	> 300	> 300	290	> 300	NE	1	1
18*[d]		NO_2		OCH_3			> 300	> 300	152	168	178	NE	2	1
19*[d]		NO_2			OCH_3		> 300	262	205	186	> 300	NE	2	2
20*[d]		NO_2				OCH_3	> 300	> 300	> 300	> 300	> 300	NE	1	1
21*[d]			NO_2	OCH_3			> 300	> 300	143	125	223	NE	2	2
22*[d]			NO_2		OCH_3		> 300	> 300	> 300	> 300	> 300	NE	1	1
3*[d]			NO_2			OCH_3	4	7	4	5	14	NE	1	3

[a] IC_{50} values in μM were determined by fitting the Hill equation to average composite concentration−effect curves from 3−17 oocytes injected with NR1/NR2A, NR1/NR2B, NR1/NR2C, NR1/NR2D, GluR1, or GluR6 cRNA. Oocytes were obtained from 1−3 frogs; NE indicates no effect. IC_{50} values greater than 300 μM were determined as described in the Experimental Methods. [b] (IC_{50} NR2A)/(IC_{50} NR2D). [c] (IC_{50} GluR1)/(IC_{50} NR2D). [d] *1−10 mM 2-hydroxypropyl-β-cyclodextrin was included for 30 and 100 μM concentrations of test compound. See Figure S2 (Supporting Information) for full general structure.

Table 2. Optimization of Subunit Selectivity through Evaluation of Ring A Substituents[a]

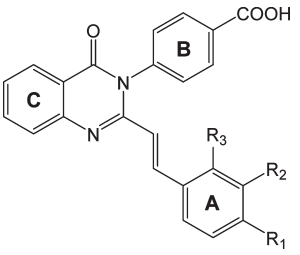

no.	R_1	R_2	R_3	NR2A IC_{50}	NR2B IC_{50}	NR2C IC_{50}	NR2D IC_{50}	GluR1 IC_{50}	NR2A[b]/NR2D	GluR1[c]/NR2D
23				84	85	39	33	25	3	1
24	OCH_3			100	98	42	31	250	3	8
25		OCH_3		24	36	17	9	27	3	3
26			OCH_3	88	51	32	16	38	6	2
27	CF_3			61	55	23	15	233	4	16
28		CF_3		13	26	8	12	22	1	2
29			CF_3	> 300	> 300	88	28	> 300	> 10	> 10
30	OH			38	35	50	36	110	1	3
31		OH		52	30	24	17	24	3	1
32			OH	20	18	20	18	36	1	2
7	NO_2			64	93	15	15	> 300	4	> 20
2		NO_2		21	30	12	9	32	2	4
13			NO_2	11	17	8	6	6	2	1
33	CH_3			41	138	28	17	> 300	2	> 17
34		CH_3		21	34	28	18	> 300	1	> 16
35			CH_3	86	93	80	81	62	1	1

[a] IC_{50} values in μM were determined by fitting the Hill equation to average composite concentration−effect curves from 4−17 oocytes injected with NR1/NR2A, NR1/NR2B, NR1/NR2C, NR1/NR2D, or GluR1 cRNA. Oocytes were obtained from 1−3 frogs. Compounds **2** and **7**, previously shown in Table 1, are included here to facilitate comparison. IC_{50} values greater than 300 μM were determined as described in the Experimental Methods. [b] (IC_{50} NR2A)/(IC_{50} NR2D). [c] (IC_{50} GluR1)/(IC_{50} NR2D). See Figure S2 (Supporting Information) for full general structure.

were inactive at NMDA and AMPA receptors (Figure S2 in Supporting Information), suggesting substitutions of aryl rings A and B are essential for activity. To evaluate whether we could improve the selectivity for NMDA receptors over AMPA receptors, positional isomer combinations of both **2** (A ring $R_2 = NO_2$, B ring $R_4 =$ COOH) and **3** (A ring $R_3 = NO_2$, B ring $R_6 =$ OMe) were evaluated (Table 1). All positional isomer modifications of A and B ring substitution led to significantly decreased potency (increased IC_{50}) compared to the screening hit **3**, and thus no further work was conducted within this series. Two positional isomeric analogues of compound **2** appeared to inhibit NR1/NR2D responses with IC_{50} values of 15 μM (**7**) and 6 μM (**13**). Notably, **2**, **7**, and **13** all contained a *para*-carboxylic acid B ring substituent despite differential *ortho*-, *meta*-, or *para*-substitution of the A ring nitro group. This suggested optimal placement of the *para*-carboxylic acid B ring substituent would likely yield the most active analogues within this structural series. Moreover, a number of these compounds showed improved selectivity for NMDA receptors over the AMPA receptor GluR1, as well as improved selectivity for NR2D-containing NMDA receptors over receptors containing the NR2A subunit, although the substitution patterns controlling these effects were unclear. The IC_{50} values for inhibition of NR2C- and NR2D-containing receptors were more similar than those for NR2A- and NR2B-containing receptors. These initial experiments suggested that it might be possible to identify derivatives within this class that selectively inhibit NR2C/D-containing recombinant NMDA receptors compared to AMPA, kainate, or NR2A/B-containing NMDA receptors.

The Effect of Substituent Position and Identity on Rings A, B,C. To further evaluate the effects of different aryl ring substituents, we measured the fitted IC_{50} values for inhibition at recombinant NR1/NR2A, NR1/NR2B, NR1/NR2C, NR1/NR2D, and GluR1 receptor current responses under voltage clamp for each test compound. The position of a variety of A ring substituents was tested while holding the B ring substituent constant ($R_4 =$ COOH) (Table 2). Given the lack of any detectable activity at recombinant kainate receptors (Table 1), responses at GluR6 were not studied further. A ring substitution at the *meta* position (R_2) was either equipotent or modestly improved potency compared to *ortho* (R_3) or *para* (R_1) A ring substitutions at NR2D-containing receptors among all analogues tested. For example, analogues containing *meta* methoxy (**25**) and trifluoromethyl (**28**) were most potent among positional isomers, whereas *meta* and *ortho* hydroxyl (**31**, **32**) and nitro (**2**, **13**) A ring substituents had nearly equivalent potencies.

The positional preference for C ring substitutions was explored utilizing chlorinated derivatives while retaining optimal A ring ($R_2 = NO_2$) and B ring ($R_4 =$ COOH) substitutions (Table 3; Figure S2 in Supporting Information). Substitution at position R_8, specifically compound **37**, gave both improved potency (IC_{50} 1 μM) and selectivity (IC_{50} NR2A/IC_{50} NR2D = 16) for monosubstituted compounds. Interestingly, the R_8,R_{10}-dichloro compound **40** showed enhanced NR2D selectivity (IC_{50} NR2A/IC_{50} NR2D = 22) with decreased on-target potency (IC_{50} 10 μM) .

Evaluation of a series of R_8 C ring substituents revealed a correlation between van der Waals radii of the series H, F, Cl, Br, I, and both the IC_{50} value at NR1/NR2D ($r = -0.95$;

Table 3. Optimization of Subunit Selectivity through Evaluation of Ring C Substituents[a]

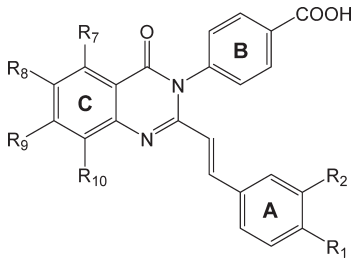

no.	R_1	R_2	R_7	R_8	R_9	R_{10}	NR2A IC_{50}	NR2B IC_{50}	NR2C IC_{50}	NR2D IC_{50}	GluR1 IC_{50}	NR2A[b]/NR2D	GluR1[c]/NR2D
36		NO_2	Cl				> 300	110	22	14	> 300	> 20	> 20
37		NO_2		Cl			16	13	2	1	7	16	7
38		NO_2			Cl		32	52	16	15	41	2	3
39[f]		NO_2				Cl	56	243	12	9	87	6	10
40		NO_2		Cl		Cl	224	109	16	10	> 300	22	30
41	NO_2			Cl		Cl	> 300	> 300	9	6	> 300	> 50	> 50
2		NO_2		H			21	30	12	9	32	2	4
42		NO_2		F			36	33	14	7	7	5	1
37		NO_2		Cl			16	13	2	1	7	16	7
43		NO_2		Br			17	13	2	1	8	17	8
44		NO_2		I			18	6	1	0.6	31	18[e]	52
45		NO_2		CH_3			12	15	5	2	27	6	14
46[f]		NO_2		OCH_3			229	> 300	6	3	> 300	76	> 100
47[f]		NO_2		NO_2			NE	NE	204	90	> 300		
48		NO_2		OH			237	> 300	43	10	96	24	10
49		NO_2		C_6H_5			11	3	2[d]	2[d]	5	6	3
50		NO_2		R_8-C_4H_4-R_9			11	5	2[d]	2[d]	4	6	2
51		NO_2		R_8-OCH_2CH_2O-R_9			> 300	> 300	281	213	> 300	1	1
52		NO_2		R_8-OCH_2O-R_9			112	162	40	36	> 300	3	> 8
53[f]		NO_2		$CH(CH_3)_2$			101	98	6	7	200	14	29
54		NO_2		$CH_2CH_2CH_3$			28	18	3	4	50	7	13
55		NO_2		2-thiophene			157	129	5	3	280	52	93
56		NO_2		$CHCHC_6H_5$			19	30	4	4	131	5	33

[a] IC_{50} values in μM were determined by fitting the Hill equation to average composite concentration−effect curves from 7−26 oocytes injected with NR1/NR2A, NR1/NR2B, NR1/NR2C, NR1/NR2D, GluR1 cRNA. Oocytes were obtained from 2−5 frogs. Compound **2**, previously shown in Table 1, is included to facilitate comparison. IC_{50} values greater than 300 μM were determined as described in Experimental Methods. NE indicates no effect. [b] (IC_{50} NR2A)/(IC_{50} NR2D). [c] (IC_{50} GluR1)/(IC_{50} NR2D). [d] Data were fitted with a variable minimum (see text). [e] Selectivity was calculated from IC_{50} values rounded to nearest value in μM. [f] *1−10 mM 2-hydroxypropyl-β-cyclodextrin was included for 30 and/or 100 μM concentrations of test compound. See Figure S2 (Supporting Information) for full general structure.

$p < 0.01$; Figure S3 in Supporting Information) and the selectivity for NR2D over NR2A ($r = 0.97$; $p < 0.01$). In particular, iodinated derivative **44** inhibited NR1/NR2D receptor responses with an IC_{50} value of 600 nM and is 18- and 52-fold selective over recombinant NR2A and AMPA GluR1 receptors, respectively (Table 3). It is unclear whether the increased potency and selectivity of **44** can be attributed to an electropositive effect or a steric effect. Consistent with a steric effect, we observed that other analogues containing large R_8 substituents also improve NR2D apparent selectivity such as R_8 = Ph (**49**) and R_8,R_9-naphthyl (**50**) when it is assumed that inhibition is complete at saturating concentrations. However, the inhibition curves with these larger hydrophobic substituents revealed incomplete inhibition. Fitting the concentration−effect data for these compounds with a variable minimum (see Experimental Methods) resulted in little difference in potency between the various NR2 subunits (see IC_{50} values in Table 3). Nevertheless, the fitted curves reveal striking differences in the degree of inhibition. For example, a saturating concentration of compound **50** is predicted to reduce responses at receptors containing NR2A, NR2B, NR2C, or NR2D to 68, 50, 26, or 20% of control, respectively. Similarly, a saturating concentration of compound **49** is predicted to reduce responses at saturating concentrations for receptors containing NR2A, NR2B, NR2C, or NR2D to 68, 51, 22, or 14% of control, respectively. These classes of compounds were not studied further.

Robust combined selectivity for NR2C and NR2D over NR2A, NR2B, and GluR1 was achieved with methoxy at the R_8 position (**46**, IC_{50} 3 μM), which was greater than 100-fold selective for NR1/NR2D over GluR1. This compound series has a maximum solubility of 70 μM ($n = 2$), necessitating the use of 1 mM β-cyclodextrin for concentrations above 70 μM. IC_{50} values for **46** at NR2C were similar to those at NR2D. Likewise, IC_{50} values at NR2A were typically similar to NR2B and were greater than 50-fold higher than at NR2C/D containing receptors (see Table 3).

We subsequently tested the effect of altering the nitro and carboxylic acid substituents on the A and B rings, respectively, for compounds where R_8 was methoxy (C ring) (Table 4). Replacement of the *p*-carboxylic acid functionality on the B ring with hydrogen (**57**), cyano (**58**), amido (**59**), or methyl ester (**60**) moieties led to compounds that were either substantially less potent or inactive (Table 4). These results

Table 4. Substitutions for Ring B Carboxylic Acid and Ring A Nitro Groups[a]

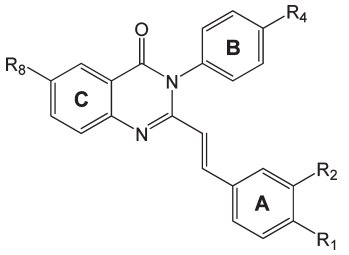

no.	R_1	R_2	R_4	R_8	NR2A IC_{50}	NR2B IC_{50}	NR2C IC_{50}	NR2D IC_{50}	GluR1 IC_{50}	NR2A[b]/NR2D	GluR1[c]/NR2D
57[d]		NO_2			> 300	> 300	> 300	> 300	> 300	1	1
46[d]		NO_2	COOH	OCH_3	229	> 300	6	3	> 300	76	> 100
58		NO_2	CN	OCH_3	> 300	> 300	> 300	> 300	> 300	1	1
59		NO_2	$CONH_2$	OCH_3	> 300	82	58	> 300	> 300	1	1
60		NO_2	$COOCH_3$	OCH_3	218	46	39	38	138	6	4
61		OCH_3	COOH	OCH_3	73	109	18	9	220	8	24
62		COOH	COOH	OCH_3	> 300	> 300	> 300	131	> 300	> 2	> 2
63		$COOCH_3$	COOH	OCH_3	80	39	15	6	41	13	7
64	$COOCH_3$	$COOCH_3$	COOH	OCH_3	> 300	> 300	124	52	> 300	> 6	> 6
7	NO_2		COOH		64	93	15	15	> 300	4	> 20
65	SCH_3		COOH		211	79	42	22	244	10	11
66	CN		COOH		94	106	28	34	> 300	3	> 9
67	$N(CH_3)_2$		COOH		> 300	> 300	63	53	> 300	> 5	> 5
68	$OCHF_2$		COOH		73	89	33	22	208	3	9
69	OCH_2CHCH_2		COOH		> 300	144	111	30	> 300	> 10	> 10
70	OCH_2COOH		COOH		> 300	> 300	> 300	> 300	> 300	1	1
71	COOH		COOH		> 300	> 300	> 300	> 300	> 300	1	1

[a] IC_{50} values in μM were determined by fitting the Hill equation to average composite concentration−effect curves from 4−26 oocytes injected with NR1/NR2A, NR1/NR2B, NR1/NR2C, NR1/NR2D, GluR1 cRNA. Oocytes were obtained from 1−4 frogs. Compounds **7** and **46**, previously shown in Table 3, are included to facilitate comparison. IC_{50} values greater than 300 μM were determined as described in the Experimental Methods. [b] (IC_{50} NR2A)/(IC_{50} NR2D). [c] (IC_{50} GluR1)/(IC_{50} NR2D). [d] *1−10 mM 2-hydroxypropyl-β-cyclodextrin was included for 100 μM concentrations of test compound. See Figure S2 (Supporting Information) for full general structure.

suggest an anionic component such as the carboxylate is crucial for binding. Substitutions of the A ring nitro group that maintained some activity included R_2 = OMe (**61**, NR2D IC_{50} 9 μM) and R_2 = $COOCH_3$ (**63**, NR2D IC_{50} 6 μM). Only modest activity was maintained with *para* substituents on the A ring (Table 4). These data suggest the binding pocket prefers the electron rich nitro and carboxylic acid groups on rings A and B, respectively.

Although compounds with R_2 = NO_2 (**2**) or R_3 = NO_2 (**13**) A ring substitution gave the best potency, improved selectivity for NMDA over AMPA receptors was noted for R_1 = NO_2 analogues (**7** and **8** in Table 1), as well as modestly improved selectivity for NR2D over NR2A with R_5 = COOH B ring substitution (**11** in Table 1). This led to a systematic comparison of ring substituents among these two positions (A ring: R_1, R_2 = NO_2; B ring: R_4, R_5 = COOH) for the most potent and selective ring C substitutions where R_8 was iodo or methoxy. Table 5 summarizes data describing these compounds, fitted as described in the Experimental Methods. The best potency was obtained for compounds with *para*-carboxylic acid substitution on the B ring (R_4 = COOH), in particular compounds **44**, **46** (Figure 2A). Among iodo-substituted compounds, **72**, which contains a *para*-nitro A ring (R_1 = NO_2), inhibited NR2C/D containing receptors with the best apparent selectivity over NR2A, NR2B, or AMPA receptors. We similarly saw somewhat improved selectivity with *para*-nitro in compound **41** (Table 3). Compound **72** had a maximum solubility of 10 μM and thus required addition of 1 mM 2-hydroxypropyl-β-cyclodextrin at concentrations above 10 μM. We were unable to determine an IC_{50} value for NR2A, NR2B, and GluR1 AMPA receptors, but this value would theoretically be greater than 300 μM given the level of inhibition observed at 100 μM of compound **72**. Inhibition by **72** at NR1/NR2C and NR1/NR2D was incomplete, leading us to fit the data with a variable minimum (see Experimental Methods), which was on average 31% and 26% of control, respectively (Figure 2B).

Effect of Changes to the Backbone on Subunit Selectivity and Potency at NR2C/D Receptors. Modifications to the styryl A ring linker were also explored to determine the nature of the backbone structure in terms of both potency and subunit selectivity (Table 6). Complete removal of the ring, as in compound **78**, which contains merely the quinazolin-4-one core structure, resulted in a total loss of inhibitory activity at concentrations up to 100 μM. We further investigated the saturation level of the styryl linker between the A ring and the quinazolin-4-one core structure. Reduction of the styryl linker of **80** (no A ring substitutions, B ring *p*-carboxylic acid, C ring R_8 methyl; IC_{50} 26 μM) to the fully saturated linker analogue **81** (fitted IC_{50} 282 μM; Table 6) resulted in 10-fold potency reduction. These data suggest the geometry of the *trans*-alkene linker is preferred for activity. Incorporation of larger ring systems pendant to the C ring led to compounds with modest activity, as shown by the various napthyl derivatives (**82**, **83**, and **84**) and phenyl-1,4-dioxane (**86**; Table 6), suggesting the presence of an extended space in the binding pocket for larger hydrophobic groups. Replacement of the A ring with a 3-pyridyl system also produced active compounds. The 3-pyridyl A ring analogues

Table 5. Optimization of Ring A, Ring B, Ring C Substituents[a]

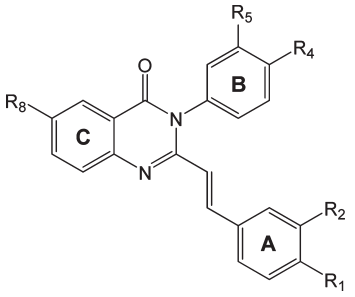

no.	R_1	R_2	R_4	R_5	R_8	NR2A IC_{50}	NR2B IC_{50}	NR2C IC_{50}	NR2D IC_{50}	GluR1 IC_{50}	NR2A[b] / NR2D	GluR1[c] / NR2D
72[e]	NO_2		COOH		I	> 300	> 300	2[d]	1[d]	> 300	> 150	> 220
44		NO_2	COOH		I	18	6	1	0.6	31	30	52
73	NO_2			COOH	I	> 300	279	9	8	> 300	> 37	> 37
74		NO_2		COOH	I	8	11	2	1	21	8	21
75	NO_2		COOH		OCH_3	197	206	13	7	> 300	28	> 42
46[e]		NO_2	COOH		OCH_3	229	> 300	6	3	> 300	76	> 100
76	NO_2			COOH	OCH_3	238	238	21	16	> 300	15	> 19
77		NO_2		COOH	OCH_3	208	> 300	24	13	289	16	22

[a] IC_{50} values in μM were determined by fitting the Hill equation to average composite concentration−effect curves from 7−26 oocytes injected with NR1/NR2A, NR1/NR2B, NR1/NR2C, NR1/NR2D, GluR1 cRNA. Oocytes were obtained from 2−5 frogs. Compounds **44** and **46**, previously shown in Table 3, are included to facilitate comparison. IC_{50} values greater than 300 μM were determined as described in the Experimental Methods. [b] (IC_{50} NR2A)/(IC_{50} NR2D). [c] (IC_{50} GluR1)/(IC_{50} NR2D). [d] Indicates data fitted with variable minimum (see Figure 2B). [e] *1 mM 2-hydroxypropyl-β-cyclodextrin was included for 30 and/or 100 μM concentrations of test compound. See Figure S2 (Supporting Information) for full general structure.

with the most potent C ring substitution (R_8 = iodine; Table 7) were subsequently evaluated. Compound **91** (R_6 = OMe) exhibited reasonable potency (IC_{50} 2.5 μM) with modest selectivity (10-fold) over NR2A and good selectivity over GluR1 (66-fold). Introduction of a carboxylic acid at position R_4 (**98**) or R_5 (**99**) gave reasonable potency; however, selectivity over GluR1 was more modest.

Discussion and Conclusions

These data show that a previously unknown and novel binding site exists on recombinant NMDA receptors expressed in heterologous systems at which modulators can act with clear preference for NR2C/D subunits. The two most potent and selective compounds in terms of inhibition of NR2C/D-containing receptors to emerge from these experiments are compounds **46** and **72** (Figure 2). Both **46** and **72** are highly selective for NMDA receptors over GluR6 kainate receptors. Compound **46** is over 50-fold selective for NR2D over NR2A/B and at least 100-fold selective over GluR1. Compound **72** also appears to be selective over NR2A/B-containing receptors. Figure 2 compares the concentration−effect curves for each of these compounds at five different glutamate receptors. Overall, a small subset of compounds within this class is characterized by poor aqueous solubility at or above 100 μM. Thus, the compounds discussed here may be more selective than we have conservatively reported. These compounds represent the first set of noncompetitive antagonists with selectivity for recombinant NMDA receptors containing NR2C/D subunits over receptors containing NR2A/B subunits. These data suggest that native NMDA receptors may have binding sites for this class of modulators, and that the concentration−effect relationship associated with this class of compounds may show significant differences between the NR2A/B and NR2C/D receptors. Thus, this class of molecules may serve as a starting point for the development of potent and subunit-selective NMDA receptor inhibitors.

Experimental Methods

Biology Experimental. Two-Electrode Voltage-Clamp Electrophysiology. Two-electrode voltage-clamp recordings were performed on *Xenopus* oocytes expressing recombinant rat NR1/NR2A, NR1/NR2B, NR1/NR2C, NR1/NR2D, GluR1, or GluR6 receptors. cDNAs for rat NR1−1a (GenBank accession numbers U11418 and U08261; hereafter NR1), NR2A (D13211), NR2B (U11419), NR2C (M91563), NR2D (L31611), GluR1 (X17184), GluR6 (Z11548) were provided by Drs. S. Heinemann (Salk Institute), S. Nakanishi (Kyoto University), and P. Seeburg (University of Heidelberg). Oocyte isolation and RNA injection were completed as described in detail elsewhere;[59] all protocols involving *Xenopus laevis* were approved by the Emory University Institutional Animal Care and Use Committee. During two-electrode voltage-clamp recordings, oocytes were placed into a perfusion chamber and continually washed with recording solution containing (in mM) 90 NaCl, 1.0 KCl, 0.5 $BaCl_2$, 0.005 EDTA, and 10 HEPES at pH 7.4 (23 °C). Glass electrodes with a tip resistance of 0.5−2.5 MΩ were pulled from thin-walled glass capillary tubes and filled with 0.3−3.0 M KCl. An OC-725C amplifier (Warner Instrument Co) was used to hold the membrane potential of the oocytes at −40 mV during current recording. All compounds were made as 20 mM stock solutions in DMSO and dissolved to reach the desired final concentration in recording solution containing 100 μM glutamate and 30 μM glycine for use on oocytes expressing NMDA receptors. Final DMSO content was 0.05−0.5% (v/v). Oocytes expressing GluR6 receptors were pretreated with 10 μM concanavalin A for 10 min. Recombinant GluR1 and GluR6 receptors were activated by 100 μM glutamate. To prevent a gradual increase in current response over the course of the experiment, which appears to be a common feature of NR1/NR2A receptor responses in oocytes, some oocytes expressing NR1/NR2A were either pretreated with 50 μM BAPTA-AM (1,2-bis(*o*-aminophenoxy)ethane-*N*,*N*,*N*′,*N*′-tetraacetic acid tetraacetoxymethyl ester) for 10 min or injected with 50 nL of 2 mM K-BAPTA (potassium 1,2-bis(*o*-aminophenoxy)ethane-*N*,*N*,*N*′,*N*′-tetraacetic acid).

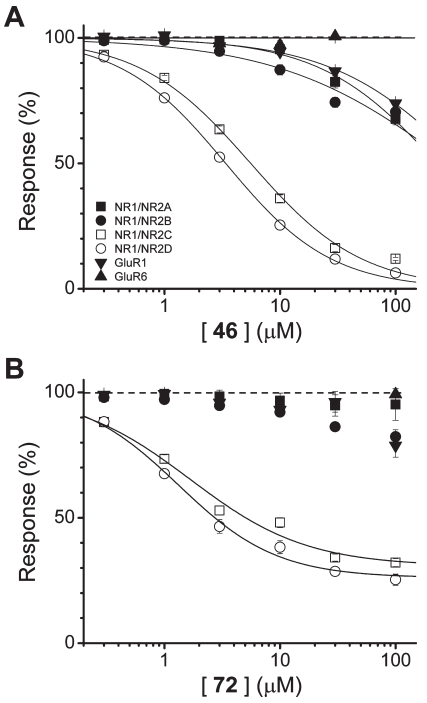

Figure 2. Mean composite concentration−effect curves are shown for NR1/NR2A, NR1/NR2B, NR1/NR2C, NR1/NR2D, GluR1, GluR6 for compounds (A) **46** and (B) **72**; error bars are SEM. 2-Hydroxypropyl-β-cyclodextrin (1 mM) was included in solutions of 30 and 100 μM **72** and 100 μM for **46**. For compound **46**, recordings of NMDA and AMPA receptor responses were made from 16 to 28 oocytes per receptor; oocytes were isolated from 3−5 different frogs. For compound **72**, recordings of NMDA and AMPA receptor responses were made from 11−15 oocytes from 3 batches of oocytes from different frogs. No significant effect was observed for 30 μM **46** or **72** on GluR6 responses (6 oocytes, 1−2 batches of oocytes from different frogs for each compound).

For every test compound, we recorded 5−7 concentrations in at least 4 oocytes per concentration on each of five different receptors. We subsequently determined the IC_{50} (half-maximally effective concentration of inhibitor) by fitting the equation

$$\text{response} = (100 - \text{minimum})/(1 + ([\text{I}]/\text{IC}_{50})^{N}) + \text{minimum} \quad (1)$$

to the mean composite concentration−response data normalized to the response in the absence of inhibitor (100%). N is the Hill slope, [I] is the inhibitor concentration, and minimum is the residual inhibition at saturating concentrations of ligand. Because inhibition was complete for most compounds tested, the minimum was fixed to 0 for all fitted curves unless otherwise indicated. For a few compounds with bulky hydrophobic C ring substituents (**49**, **50**, **72**), minimum was allowed to vary. Compounds that showed a response greater than 75% of control in the presence of 100 μM test compound are reported as having an IC_{50} value > 300 μM, which is theoretically predicted by the Hill equation for a slope of 1.

The maximum solubility was determined in a subset of 24 compounds representing various classes of structure using a BMG Labtech Nephelostar nephelometer (Offenburg, Germany) according to manufacturer's instructions. Maximum solubility of each test compound was determined in oocyte recording solution (components given below) and 1% DMSO. Only responses for concentrations below the experimentally determined limit of solubility were measured; whenever necessary, we repeated experiments with 1−10 mM 2-hydroxypropyl-β-cyclodextrin added to the recording solution to ensure that the compounds remained in solution up to 100 μM. 2-Hydroxypropyl-β-cyclodextrin had no detectable effect on NMDA response amplitude (data not shown).

Chemistry Experimental. Compounds not described below were purchased from commercial vendors. Provided samples were of greater than 90% purity, as determined by the suppliers, via HPLC or NMR.

All reagents were obtained from commercial suppliers and used without further purification. Reaction progress was monitored by thin layer chromatography (TLC) on precoated glass plates (silica gel 60 F254, 0.25 mm). Proton and carbon NMR spectra were recorded on an INOVA-400 (400 MHz), VNMRS 400 (400 MHz), INOVA-600 (600 MHz), or Mercury 300 Vx (300 MHz). The spectra obtained were referenced to the residual solvent peak. Mass spectra were performed by the Emory University Mass Spectroscopy Center on either a VG 70-S Nier Johnson or JEOL instrument. Elemental analyses were performed by Atlantic Microlab Inc. C, H, N agreed with proposed structures within ±0.4% of theoretical values unless indicated. Flash chromatography was performed on a Teledyne ISCO Combiflash Companion with prepackaged Teledyne RediSep disposable normal phase silica columns. Melting temperatures were determined on a Mel-Temp apparatus and are uncorrected.

General Procedure for Synthesis of (*E*)-3-Phenyl-2-styrylquinazolin-4(3*H*)-one Products (Procedure C). The quinazolinone (**6**, 1.0 equiv), benzaldehyde (1.33 equiv), and sodium acetate (1.63 equiv) were suspended in a mixture of glacial acetic acid (58 equiv) and acetic anhydride (7.0 equiv). The mixture was refluxed until TLC indicated the reaction was finished (generally 12−18 h). After cooling to room temperature, the mixture was filtered and washed with methanol. Further purification was performed (chromatography or recrystallization) as necessary.

(*E*)-4-(2-(3-Nitrostyryl)-4-oxoquinazolin-3(4*H*)-yl)benzoic Acid (2). Compound **2** was prepared via procedure C with compound **2b** (0.100 g, 0.36 mmol) and *meta*-nitrobenzaldehyde (0.072 g, 0.48 mmol, 1.3 equiv). The crude material was purified via silica gel chromatography (ISCO, RediSep 12 g column, silica cake, 5−10% MeOH/DCM gradient) to give an off-white solid (0.030 g, 20%). ^{1}H NMR (600 MHz, DMSO-d_6) δ 8.26 (s, 1H), 8.17 (d, J = 7.6 Hz, 4H), 8.01 (d, J = 15.2 Hz, 1H), 7.92 (t, J = 7.1 Hz, 1H), 7.86 (d, J = 7.6 Hz, 1H), 7.81 (d, J = 8.1 Hz, 1H), 7.65−7.62 (mult, 3H), 7.58 (t, J = 7.6 Hz, 1H), 6.51 (d, J = 15.7 Hz, 1H). ^{13}C NMR (150 MHz, DMSO-d_6) δ 166.7, 161.1, 150.6, 148.3, 147.2, 140.7, 136.7, 136.6, 135.0, 133.3, 131.6, 130.6, 130.5, 129.5, 127.4, 127.1, 126.5, 124.0, 122.8, 122.4, 120.7, 103.3. HRMS calcd for $C_{23}H_{15}N_3O_5$, 414.10911 $[M + H]^+$; found, 414.10791 $[M + H]^+$. Anal. ($C_{23}H_{15}N_3O_5 \cdot 0.25$AcOH) C, H, N. MP > 260 °C.

(*E*)-2-(2-(4-Nitrostyryl)-4-oxoquinazolin-3(4*H*)-yl)benzoic Acid (9). Compound **9** was prepared via procedure C with compound **9b** (1.00 g, 3.57 mmol) and *para*-nitrobenzaldehyde (0.717 g, 4.75 mmol, 1.33 equiv) to give the title compound as a yellow solid (1.18 g, 80%). ^{1}H NMR (400 MHz, DMSO-d_6) δ 8.20−8.14 (mult, 4H), 7.96 (d, J = 15.9 Hz, 1H), 7.92−7.81 (mult, 3H), 7.74 (t, J = 7.6 Hz, 1H), 7.68 (d, J = 7.9 Hz, 2H), 7.61−7.56 (mult, 2H), 6.50 (d, J = 15.6 Hz, 1H). ^{13}C NMR (100 MHz, DMSO-d_6) δ 165.7, 161.3, 151.0, 147.5, 147.3, 141.2, 136.6, 136.5, 134.9, 133.8, 131.8, 130.7, 130.0, 128.6, 127.4, 127.0, 126.5, 124.1, 124.0, 120.7. HRMS calcd for $C_{23}H_{15}N_3O_5$, 414.10911 $[M + H]^+$; found, 414.10903 $[M + H]^+$. Anal. ($C_{23}H_{15}N_3O_5$) C, H, N. MP > 260 °C.

***tert*-Butyldimethylsilyl 4-(6-Iodo-2-methyl-4-oxoquinazolin-3(4*H*)-yl)benzoate (10).** Carboxylic acid **78** (0.300 g, 0.74 mmol) was dissolved in THF (10.0 mL). To this solution was added *N*-methylmorpholine (0.081 mL, 0.74 mmol, 1.0 equiv) and TBDMSCl (0.111 g, 0.74 mmol, 1.0 equiv). The mixture was stirred at room temperature for 1 h. The yellow suspension was concentrated in vacuo, and the resulting residue was partitioned between ethyl acetate and water. The mixture was extracted 3× with ethyl acetate. The combined organics were washed with brine, dried over $MgSO_4$, and concentrated in vacuo to give a white solid. The crude material was purified using silica gel chromatography (ISCO, RediSep 12 g column, 100% EtOAc) to give a white foam (0.280 g, 73%).

Table 6. Optimization of the Linker and Ring A[c]

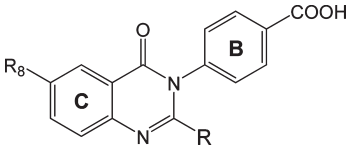

Number	R	R_8	NR2A IC_{50}	NR2B IC_{50}	NR2C IC_{50}	NR2D IC_{50}	GluR1 IC_{50}	NR2A[a] / NR2D	GluR1[b] / NR2D
78	CH_3	I	>300	>300	>300	>300	>300	1	1
79	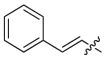	I	53	66	13	4	23	13	6
80	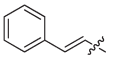	CH_3	39	25	22	26	21	2	1
81	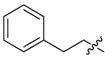	CH_3	>300	78	184	282	>300	1	1
82	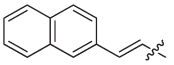		21	31	14	6	>300	4	>50
83	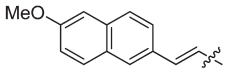		63	36	20	11	103	6	9
84	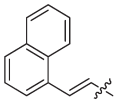		25	68	22	6	82	4	14
85	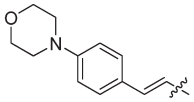		>300	122	284	171	>300	1	1
86[d]	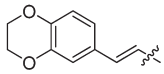		>300	262	26	16	>300	>18	>18

[a] (IC_{50} NR2A)/(IC_{50} NR2D) [b] (IC_{50} GluR1)/(IC_{50} NR2D) [c] IC_{50} values in μM were determined by fitting the Hill equation to average composite concentration−effect curves from 3−12 oocytes injected with NR1/NR2A, NR1/NR2B, NR1/NR2C, NR1/NR2D, GluR1 cRNA. Oocytes were obtained from 1−2 frogs. IC_{50} values greater than 300 μM were determined as described in the Experimental Methods. [d] 2−4 mM 2-hydroxypropyl-β-cyclodextrin was included for 1−100 μM concentrations of test compound. See Figure S2 (Supporting Information) for full general structure.

^{1}H NMR (400 MHz, $CDCl_3$) δ 8.57 (d, J = 2.1 Hz, 1H), 8.23 (d, J = 8.8 Hz, 2H), 8.02 (dd, J_1 = 8.7 Hz, J_2 = 2.1 Hz, 1H), 7.41 (d, J = 8.6 Hz, 1H), 7.34 (d, J = 8.8 Hz, 2H), 2.22 (s, 3H), 1.05 (s, 9H), 0.41 (s, 6H). ^{13}C NMR (100 MHz, $CDCl_3$) δ 165.5, 160.8, 154.3, 146.9, 143.7, 141.5, 135.9, 132.9, 132.1, 129.0, 128.4, 122.5, 91.3, 25.8, 24.6, 18.0, −4.6. HRMS calcd for $C_{22}H_{25}IN_2O_3Si$, 521.07585 $[M + H]^+$; found, 521.07527 $[M + H]^+$.

(*E*)-2-(2-(3-Nitrostyryl)-4-oxoquinazolin-3(4*H*)-yl)benzoic Acid (12). Compound **12** was prepared via procedure C with compound **9b** (0.250 g, 0.89 mmol) and *meta*-nitrobenzaldehyde (0.179 g, 1.19 mmol, 1.33 equiv) to give the title compound as a yellow solid (0.202 g, 55%). ^{1}H NMR (400 MHz, DMSO-d_6) δ 8.22−8.13 (mult, 4H), 7.99 (d, J = 15.2 Hz, 1H), 7.93−7.80 (mult, 4H), 7.75 (t, J = 7.3 Hz, 1H), 7.65−7.60 (mult, 2H), 7.57 (t, J = 7.0 Hz, 1H), 6.47 (d, J = 15.6 Hz, 1H). ^{13}C NMR (150 MHz, DMSO-d_6) δ 165.7, 161.3, 151.1, 148.3, 147.4, 136.6, 136.6, 136.6, 134.9, 133.8, 133.3, 131.8, 130.7, 130.5, 129.9, 129.4, 127.3, 126.8, 126.5, 124.0, 122.6, 122.1, 120.7. HRMS calcd for $C_{23}H_{15}N_3O_5$, 414.10911 $[M + H]^+$; found, 414.10822 $[M + H]^+$. Anal. ($C_{23}H_{15}N_3O_5$) C, H, N. MP > 260 °C.

(*E*)-4-(5-Chloro-2-(3-nitrostyryl)-4-oxoquinazolin-3(4*H*)-yl)benzoic Acid (36). Compound **36** was prepared via procedure C using compound **36b** (0.300 g, 0.95 mmol) and *meta*-nitrobenzaldehyde (0.192 g, 1.27 mmol, 1.33 equiv) to give the title compound as a bright-yellow solid (0.251 g, 59%). ^{1}H NMR (400 MHz, DMSO-d_6) δ 13.31 (bs, 1H), 8.22 (s, 2H), 8.19−8.15 (mult, 2H), 7.99 (d, J = 15.7 Hz, 1H), 7.83−7.78 (mult, 2H), 7.65 (d, J = 8.6 Hz, 2H), 7.61 (t, J = 7.8 Hz, 2H), 7.55 (d, J = 7.4 Hz, 1H), 6.42 (d, J = 15.7 Hz, 1H). ^{13}C NMR (100 MHz, DMSO-d_6) δ 166.7, 159.1, 151.2, 149.7, 148.2, 140.6, 137.3, 136.3, 134.7, 133.3, 132.9, 131.6, 130.7, 130.5, 129.5, 129.3, 126.9, 124.1, 122.4, 122.3, 117.6. HRMS calcd for $C_{23}H_{14}ClN_3O_5$, 448.07014 $[M + H]^+$; found, 448.06970 $[M + H]^+$. Anal. ($C_{23}H_{14}ClN_3O_5$) C, H, N. MP > 260 °C.

(*E*)-4-(6-Chloro-2-(3-nitrostyryl)-4-oxoquinazolin-3(4*H*)-yl)benzoic Acid (37). Compound **37** was prepared via procedure C using **37b** (0.300 g, 0.950 mmol) and *meta*-nitrobenzaldehyde (0.192 g, 1.30 mmol, 1.33 equiv). The crude material was purified using recrystallization with methanol and dioxane. Further trituration with water yielded the title compound as a yellow solid (0.060 g, 14%). ^{1}H NMR (400 MHz, DMSO-d_6) δ 8.24 (s, 1H), 8.19−1.66 (mult, 3H), 8.05 (d, J = 2.2 Hz, 1H), 8.01 (d, J = 15.6 Hz, 1H), 7.94 (dd, J_1 = 8.7 Hz, J_2 = 2.2 Hz, 1H), 7.85−7.81 (mult, 2H), 7.66−7.61 (mult, 3H), 6.48 (d, J = 15.6 Hz, 1H). ^{13}C NMR (100 MHz, DMSO-d_6) δ 167.4, 160.9, 151.8, 148.9, 146.6, 141.0, 137.9, 137.1, 135.7, 134.0, 133.0, 132.4, 131.9, 131.4, 131.8, 130.2, 130.0, 126.1, 124.8, 123.1, 122.6. HRMS calcd for $C_{23}H_{14}ClN_3O_5$, 446.05426 $[M - H]^+$; found, 446.05511 $[M - H]^+$. Anal. ($C_{23}H_{14}ClN_3O_5 \cdot 0.75H_2O$) C, H, N. MP > 260 °C.

(*E*)-4-(7-Chloro-2-(3-nitrostyryl)-4-oxoquinazolin-3(4*H*)-yl)benzoic Acid (38). Compound **38** was prepared via procedure C using compound **38b** (0.200 g, 0.640 mmol) and *meta*-nitrobenzaldehyde (0.128 g, 0.850 mmol, 1.33 equiv) to give the title compound as a yellow solid (0.135 g, 47%). ^{1}H NMR (400 MHz, DMSO-d_6) δ 8.24 (s, 1H), 8.18−8.13 (mult, 4H), 8.00 (d, J = 15.6 Hz, 1H), 7.85 (d, J = 8.3 Hz, 1H), 7.83 (d, J = 1.9 Hz, 1H), 7.65 (d, J = 8.6 Hz, 3H), 7.60 (dd, J_1 = 8.3 Hz, J_2 = 1.9 Hz, 1H). ^{13}C NMR (100 MHz, DMSO-d_6) δ 166.7, 160.6, 152.0, 148.3, 148.2, 140.4, 139.5, 137.6, 136.3, 133.4, 131.7, 130.7, 130.6, 130.5, 129.4, 128.6, 127.2, 126.3, 124.2, 122.4, 119.5 HRMS calcd for $C_{23}H_{14}ClN_3O_5$, 448.07014 $[M + H]^+$; found, 448.06890 $[M + H]^+$. Anal. ($C_{23}H_{14}ClN_3O_5$) C, H, N. MP > 260 °C.

Table 7. Optimization of Ring B Substituents for Pyridinyl Analogues[a]

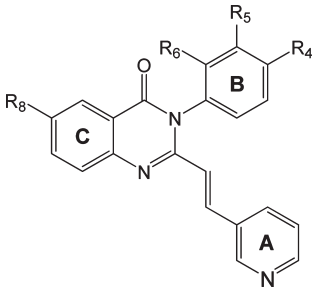

no.	R_4	R_5	R_6	R_8	NR2A IC_{50}	NR2B IC_{50}	NR2C IC_{50}	NR2D IC_{50}	GluR1 IC_{50}	$\frac{IC_{50}NR2A}{IC_{50}NR2D}$	$\frac{IC_{50}GluR1}{IC_{50}NR2D}$
87					40	51	140	35	74	1	2
88				I	132	> 300	> 300	108	> 300	1	3
89[b]	OCH_3			I	> 300	> 300	> 300	> 300	> 300	1	1
90[b]		OCH_3		I	> 300	> 300	> 300	200	> 300	1	1
91[b]			OCH_3	I	31	30	3	3	199	10	66
92[b]	CH3			I	> 300	> 300	> 300	> 300	> 300	1	1
93[b]		CH3		I	> 300	> 300	241	> 300	> 300	1	1
94[b]			CH3	I	> 300	156	70	25	83	12	3
95[b]	NO2			I	> 300	> 300	204	218	> 300	1	1
96[b]		NO2		I	> 300	> 300	> 300	> 300	> 300	1	1
97[b]			NO2	I	206	105	19	5	> 300	41	60
98	COOH			I	26	31	6	4	61	7	15
99		COOH		I	45	49	7	4	64	11	16

[a] IC_{50} values in μM were determined by fitting the Hill equation to average composite concentration−effect curves from 3−20 oocytes injected with NR1/NR2A, NR1/NR2B, NR1/NR2C, NR1/NR2D, GluR1 cRNA. Oocytes were obtained from 1−3 frogs. IC_{50} values greater than 300 μM were determined as described in the Experimental Methods. [b] 1−10 mM 2-hydroxypropyl-β-cyclodextrin was included for 10, 30, and/or 100 μM concentrations of test compounds. See Figure S2 (Supporting Information) for full general structure.

(*E*)-4-(8-Chloro-2-(3-nitrostyryl)-4-oxoquinazolin-3(4*H*)-yl)-benzoic Acid (39). Compound **39** was prepared via procedure C using compound **39b** (0.400 g, 1.27 mmol) and *meta*-nitrobenzaldehyde (0.255 g, 1.69 mmol, 1.33 equiv) to yield the title compound as a yellow solid (0.071 g, 12%). ^{1}H NMR (400 MHz, DMSO-d_6) δ 13.24 (bs, 1H), 8.26 (s, 1H), 8.17 (d, J = 8.2 Hz, 3H), 8.10−8.02 (mult, 3H), 7.86 (d, J = 7.8 Hz, 1H), 7.67−7.62 (mult, 3H), 7.53 (t, J = 7.8 Hz, 1H), 6.51 (d, J = 15.6 Hz, 1H). ^{13}C NMR (100 MHz, DMSO-d_6) δ1 67.3, 161.4, 151.9, 148.9, 144.3, 141.0, 138.4, 137.0, 135.5, 134.0, 132.3, 131.5, 131.4, 131.1, 130.0, 127.9, 126.2, 124.8, 123.2, 123.0. HRMS calcd for $C_{23}H_{14}ClN_3O_5$, 448.07014 $[M + H]^+$; found 448.07015 $[M + H]^+$. Anal. ($C_{23}H_{14}ClN_3O_5$) C, H, N. MP > 260 °C.

(*E*)-4-(6,8-Dichloro-2-(3-nitrostyryl)-4-oxoquinazolin-3(4*H*)-yl)-benzoic Acid (40). Compound **40** was prepared via procedure C using **41b** (0.250 g, 0.716 mmol) and *meta*-nitrobenzaldehyde (0.144 g, 0.952 mmol, 1.3 equiv) to give the title compound as a yellow solid, which was obtained by filtration (0.139 g, 40%). ^{1}H NMR (400 MHz, DMSO-d_6) δ 13.34 (bs, 1H), 8.29 (s, 1H), 8.24 (d, J = 2.4 Hz, 1H), 8.16−8.20 (m, 3H), 8.08 (s, 1H), 8.04−8.05 (m, 1H) 7.88 (d, J = 7.8 Hz, 1H), 7.62−7.78 (m, 3H), 6.51 (d, J = 15.6 Hz, 1H). ^{13}C NMR (100 MHz, DMSO-d_6) δ 166.7, 159.9, 151.8, 148.3, 142.8, 140.2, 138.2, 136.3, 134.5, 133.4, 131.8, 130.8, 130.7, 130.6, 129.3, 124.7, 124.3, 123.2, 122.8, 122.4. HRMS calcd for $C_{23}H_{13}Cl_2N_3O_5$, 482.03114 $[M + H]^+$; found 482.03068 $[M + H]^+$. Anal. ($C_{23}H_{13}Cl_2N_3O_5$) C, H, N. MP > 260 °C.

(*E*)-4-(6,8-Dichloro-2-(4-nitrostyryl)-4-oxoquinazolin-3(4*H*)-yl)-benzoic Acid (41). Compound **41** was prepared via procedure C using compound **41b** (0.250 g, 0.716 mmol) and *para*-nitrobenzaldehyde (0.144 g, 0.952 mmol, 1.3 equiv) to yield the title compound as a yellow solid (0.050 g, 14%). ^{1}H NMR (400 MHz, DMSO-d_6) δ 13.34 (bs, 1H), 8.24 (d, J = 2.7, 1H) 8.16−8.20 (mult, 4H), 8.05 (d, J = 2.4, 1H), 8.02 (d, J = 15.7, 1H), 7.71 (d, J = 9.0, 2H), 7.65 (d, J = 8.6, 2H), 6.53 (d, J = 15.3, 1H). ^{13}C NMR (100 MHz, DMSO-d_6) δ 166.7, 159.9, 151.6, 147.7, 142.7, 140.8, 140.1, 138.0, 134.5, 132.4, 131.8, 130.9, 130.8, 129.3, 129.0, 124.7, 124.2, 123.7, 123.2. HRMS calcd for $C_{23}H_{13}Cl_2N_3O_5$, 482.03114 $[M + H]^+$; found, 482.0974 $[M + H]^+$. Anal. ($C_{23}H_{13}Cl_2N_3O_5$) C, H, N. MP > 260 °C.

(*E*)-4-(6-Fluoro-2-(3-nitrostyryl)-4-oxoquinazolin-3(4*H*)-yl)-benzoic Acid (42). Compound **42** was prepared via procedure C using **42b** (0.400 g, 1.34 mmol) and *meta*-nitrobenzaldehyde (0.270 g, 1.78 mmol, 1.33 equiv). The crude material was purified by recrystallization with methanol and dioxane and further purification by trituration with methanol and ethyl acetate to remove residual dioxane to yield the title compound as a pale-yellow solid (0.268 h, 43%). ^{1}H NMR (600 MHz, DMSO-d_6) δ 8.24 (s, 1H), 8.18−8.16 (mult, 3H), 7.99 (d, J = 15.5 Hz, 1H), 7.89−7.80 (mult, 4H), 7.66−7.62 (mult, 3H), 6.49 (d, J = 15.7, 1H). ^{13}C NMR (100 MHz, DMSO-d_6) δ 166.7, 160.5, 159.8 (d, J = 245 Hz), 150.2, 148.3, 144.1, 140.5,136.8, 136.5, 133.3, 131.6, 130.7, 130.5, 130.3, 130.0, 129.4, 124.0, 123.3 (d, J = 24 Hz), 122.4 (d, J = 15 Hz) 121.9 (d, J = 8.4 Hz), 111.2 (d, J = 24 Hz). HRMS calcd for $C_{23}H_{14}FN_3O_5$, 432.09969 $[M + H]^+$; found, 432.09850 $[M + H]^+$. Anal. ($C_{23}H_{14}FN_3O_5$) C, H, N. MP > 260 °C.

(*E*)-4-(6-Bromo-2-(3-nitrostyryl)-4-oxoquinazolin-3(4*H*)-yl)-benzoic Acid (43). Compound **43** was prepared via procedure C using compound **43b** (0.300 g, 0.840 mmol) and *meta*-nitrobenzaldehyde (0.168 g, 1.10 mmol, 1.33 equiv). The crude material was recrystallized using methanol and dioxane and further purified by hot trituration with methanol and ethyl acetate to remove residual dioxane to yield the title compound as a yellow solid (0.120 g, 30%). ^{1}H NMR (300 MHz, DMSO-d_6) δ 8.22 (s, 1H), 8.19−8.14 (mult, 4H), 8.04 (dd, J_1 = 8.5 Hz, J_2 = 2.3 Hz, 1H), 8.00 (d, J = 2.3 Hz, 1H), 7.82 (d, J = 7.6 Hz, 1H), 7.73 (d, J = 8.5 Hz, 1H), 7.64−7.59 (mult, 3H), 6.46 (d, J = 15.5 Hz, 1H). ^{13}C NMR (100 MHz, DMSO-d_6) δ 166.8, 160.0, 151.1, 148.2, 146.1, 140.0, 137.7, 137.2, 136.4, 133.2,

132.5, 130.7, 130.5, 129.6, 129.2, 128.5, 124.1, 122.4, 122.2, 119.3. HRMS calcd for $C_{23}H_{14}BrN_3O_5$, 492.01962 $[M + H]^+$; found, 492.00228 $[M + H]^+$. Anal. ($C_{23}H_{14}BrN_3O_5$) C, H, N. MP > 260 °C.

(*E*)-4-(6-Methyl-2-(3-nitrostyryl)-4-oxoquinazolin-3(4*H*)-yl)benzoic Acid (45). Compound **45** was prepared via procedure C using compound **45b** (0.507 g, 1.72 mmol) and *meta*-nitrobenzaldehyde (0.346 g, 2.29 mmol, 1.33 equiv) to yield the title compound as a yellow solid (0.498 g, 68%). ^{1}H NMR (400 MHz, DMSO-d_6) δ 13.34 (bs, 1H), 8.22 (s, 1H), 8.18−8.14 (mult, 3H), 7.96 (d, J = 15.6 Hz, 1H), 7.93 (s, 1H), 7.83 (d, J = 7.8 Hz, 1H), 7.73−7.77 (mult, 2H), 7.64−7.60 (mult, 3H), 6.47 (d, J = 15.6 Hz, 1H), 2.48 (s, 3H). ^{13}C (100 MHz, DMSO-d_6) δ 166.7, 161.0, 149.8, 148.2, 145.2, 140.8, 136.9, 136.6, 136.3, 133.3, 131.6, 130.7, 130.5, 129.5, 127.2, 125.8, 123.9, 122.8, 122.3, 120.4, 20.9. HRMS calcd for $C_{24}H_{17}N_3O_5$, 428.12476 $[M + H]^+$; found 428.12422 $[M + H]^+$. Anal. ($C_{24}H_{17}N_3O_5$) C, H, N. MP > 260 °C.

(*E*)-4-(6-Methoxy-2-(3-nitrostyryl)-4-oxoquinazolin-3(4*H*)-yl)-benzoic Acid (46). Compound **46** was prepared via procedure C using compound **46b** (0.120 g, 0.390 mmol) and *meta*-nitrobenzaldehyde (0.078 g, 0.51 mmol, 1.3 equiv) to yield the title compound as a yellow solid (0.094 g, 55%). ^{1}H NMR (400 MHz, DMSO-d_6) δ 8.24 (s, 1H), 8.16 (d, J = 8.3 Hz, 3H), 7.94 (d, J = 15.6 Hz, 1H), 7.84 (d, J = 7.9 Hz, 2H), 7.62 (d, J = 9.8 Hz, 1H), 7.65−7.61 (mult, 3H), 7.54−7.53 (mult, 2H), 6.49 (d, J = 15.6 Hz, 1H), 3.83 (s, 3H). ^{13}C NMR (100 MHz, DMSO-d_6) δ 167.7, 161.5, 158.8, 149.2, 148.9, 142.5, 140.9, 137.4, 136.4, 133.8, 133.7, 131.2, 129.9, 129.8, 129.7, 125.2, 124.5, 123.4, 122.9, 122.2, 56.4. HRMS calcd for $C_{24}H_{17}N_3O_6$, 444.11968 $[M + H]^+$; found, 444.11849 $[M + H]^+$. Anal. ($C_{24}H_{17}N_3O_6 \cdot 0.50\ H_2O$) C, H, N. MP > 260 °C.

(*E*)-4-(6-Nitro-2-(3-nitrostyryl)-4-oxoquinazolin-3(4*H*)-yl)-benzoic Acid (47). Compound **47** was prepared via procedure C using compound **47b** (0.250 g, 0.769 mmol) and 3-nitrobenzaldehyde (0.154 g, 1.33 equiv, 1.02 mmol). The crude material was purified by recrystallization with ethyl acetate and hexanes to give a yellow solid (0.321 g, 91%). ^{1}H NMR (400 MHz, DMSO-d_6) δ 13.35 (bs, 1H), 8.84 (d, J = 3.0 Hz, 1H), 8.65 (dd, J_1 = 9.0 Hz, J_2 = 2.6 Hz, 1H), 8.32 (s, 1H), 8.15−8.21 (mult, 4H), 7.98 (d, J = 9.0 Hz, 1H), 7.91 (d, J = 8.1 Hz, 1H), 7.63−7.77 (mult, 3H), 6.54 (d, J = 15.4 Hz, 1H). ^{13}C NMR (100 MHz, DMSO-d_6) δ 166.7, 160.6, 153.9, 151.5, 148.3, 144.8, 140.0, 139.1, 136.2, 133.6, 131.9, 130.8, 130.6, 129.3, 129.0, 128.9, 124.5, 122.9, 122.6, 122.2, 120.8. HRMS calcd for $C_{23}H_{14}N_4O_7$, 459.09414 $[M + H]^+$; found 459.09363 $[M + H]^+$. Anal. ($C_{23}H_{14}N_4O_7$) C, H, N. MP > 260 °C.

(*E*)-4-(6-Hydroxy-2-(3-nitrostyryl)-4-oxoquinazolin-3(4*H*)-yl)-benzoic Acid (48). Compound **48** was prepared via procedure C using compound **48b** (0.262 g, 0.770 mmol) and *meta*-nitrobenzaldehyde (0.156 g, 1.0 mmol, 1.33 equiv). The crude material was purified by recrystallization with methanol and dioxane and further purified by hot gravity filtration after trituration with ethyl acetate and methanol (0.095 g, 29%). ^{1}H NMR (400 MHz, DMSO-d_6) δ 8.23 (s, 1H), 8.15 (d, J = 8.6 Hz, 3H), 7.90 (d, J = 15.6 Hz, 1H), 7.83 (d, J = 7.8 Hz, 1H), 7.69 (d, J = 9.0 Hz, 1H), 7.62−7.59 (mult, 3H), 7.45 (d, J = 3.1 Hz, 1H), 7.36 (dd, J_1 = 8.6 Hz, J_2 = 2.7 Hz, 1H), 6.47 (d, H = 15.7 Hz, 1H). ^{13}C NMR (100 MHz, DMSO-d_6) δ 166.7, 160.8, 156.7, 148.3, 147.6, 140.9, 140.4, 136.8, 135.3, 133.2, 131.4, 130.6, 130.5, 129.5, 129.2, 124.5, 123.7, 122.8, 122.2, 121.7, 109.4. HRMS calcd for $C_{23}H_{15}N_3O_6$, 430.10404 $[M + H]^+$; found, 430.10455 $[M + H]^+$. Anal. ($C_{23}H_{15}N_3O_6 \cdot 0.25H_2O$) C, H, N. MP > 260 °C.

(*E*)-4-(2-(3-Nitrostyryl)-4-oxo-6-phenylquinazolin-3(4*H*)-yl)-benzoic Acid (49). Compound **49** was prepared via procedure C using **49b** (0.200 g, 0.560 mmol) and *meta*-nitrobenzaldehyde (0.113 g, 0.750 g, 1.33 equiv) to yield the title compound as a yellow solid (0.210 g, 76%). ^{1}H NMR (400 MHz, DMSO-d_6) δ 8.35 (d, J = 2.0 Hz, 1H), 8.26−8.25 (mult, 1H), 8.23 (d, J = 2.3 Hz, 1H), 8.19−8.15 (mult, 3H), 8.03 (d, J = 15.7 Hz, 1H), 7.89 (d, J = 8.2 Hz, 2H), 7.86 (d, J = 7.8 Hz, 2H), 7.67−7.65 (mult, 3H), 7.53 (t, J = 7.4 Hz, 2H), 7.43 (t, J = 7.0 Hz, 1H), 6.51 (d, J = 15.7 Hz, 1H). ^{13}C NMR (100 MHz, DMSO-d_6) δ 166.8, 161.1, 150.6, 148.2, 146.5, 140.4, 138.7, 138.6, 136.8, 136.5, 133.4, 133.3, 132.2, 130.7, 130.5, 129.4, 129.2, 128.1, 126.8, 124.0, 123.7, 122.7, 122.4, 121.0. HRMS calcd for $C_{29}H_{19}N_3O_5$, 490.14044 $[M + H]^+$; found, 490.13965 $[M + H]^+$. Anal. ($C_{29}H_{19}N_3O_5$) C, H, N. MP > 260 °C.

(*E*)-4-(2-(3-Nitrostyryl)-4-oxobenzo[*g*]quinazolin-3(4*H*)-yl)-benzoic Acid (50). Compound **50** was prepared via procedure C using compound **50b** (0.250 g, 0.760 mmol) and *meta*-nitrobenzaldehyde (0.152 g, 1.01 mmol, 1.33 equiv). The crude material was purified by hot gravity filtration with methanol (0.194 g, 55%). ^{1}H NMR (400 MHz, DMSO-d_6) δ 13.31 (bs, 1H), 8.87 (s, 1H), 8.28 (s, 1H), 8.25 (mult, 2H), 8.20−8.16 (mult, 4H), 8.02 (d, J = 15.7 Hz, 1H), 7.86 (d, J = 7.8 Hz, 1H), 7.33−7.59 (mult, 5H), 6.52 (d, J = 15.7 Hz, 1H). ^{13}C NMR (100 MHz, DMSO-d_6) δ 166.8, 161.6, 149.6, 148.3, 142.6, 140.9, 136.7, 136.5, 133.3, 131.5, 131.2, 130.7, 130.5, 129.7, 129.4, 128.8, 128.0, 126.6, 124.9, 124.0, 123.0, 122.3, 119.8. HRMS calcd for $C_{27}H_{17}N_3O_5$, 464.12474 $[M + H]^+$; found, 464.125661 $[M + H]^+$. Anal. ($C_{27}H_{17}N_3O_5$) C, H, N. MP > 260 °C.

(*E*)-4-(2-(3-Nitrostyryl)-4-oxo-7,8-dihydro-[1,4]dioxino[2,3-*g*]-quinazolin-3(4*H*)-yl)benzoic Acid (51). Compound **51** was prepared via procedure C using compound **51b** (0.150 g, 0.44 mmol) and *meta*-nitrobenzaldehyde (0.089 g, 0.59 mmol, 1.33 equiv). The crude material was purified by hot gravity filtration with methanol to give a yellow solid (0.056 g, 27%). ^{1}H NMR (400 MHz, DMSO-d_6) δ 8.19 (s, 1H), 8.14 (d, J = 8.2 Hz, 1H), 8.03 (d, J = 8.2 Hz, 2H), 7.89 (d, J = 15.7 Hz, 1H), 7.75 (d, J = 7.8 Hz, 1H), 7.64 (t, J = 7.8 Hz, 1H), 7.51 (s, 1H), 7.26 (d, J = 8.2 Hz, 2H), 7.21 (s, 1H), 6.49 (d, J = 15.7 Hz, 1H), 4.44−4.38 (mult, 4H). ^{13}C NMR (100 MHz, DMSO-d_6) δ 168.1, 160.3, 149.8, 149.7, 148.3, 143.7, 142.7, 142.0, 136.8, 136.7, 135.5, 132.9, 130.6, 130.1, 127.6, 123.8, 123.0, 122.1, 115.0, 114.2, 113.4, 112.6, 64.4, 64.3. HRMS calcd for $C_{25}H_{17}N_3O_7$, 472.11459 $[M + H]^+$; found, 472.11429 $[M + H]^+$. Anal. ($C_{25}H_{17}N_3O_7$) C, H, N. MP > 260 C.

(*E*)-4-(6-(3-Nitrostyryl)-8-oxo-[1,3]dioxolo[4,5-*g*]quinazolin-7(8*H*)-yl)benzoic Acid (52). Compound **52** was prepared via procedure C using compound **52b** (0.100 g, 0.31 mmol) and *meta*-nitrobenzaldehyde (0.062 g, 0.41 mmol, 1.33 equiv). The crude material was purified by hot gravity filtration with methanol to give a yellow solid (0.048 g, 34%). ^{1}H NMR (400 MHz, DMSO-d_6) δ 8.21 (s, 1H), 8.15 (d, J = 8.6 Hz, 1H), 8.00 (d, J = 8.3 Hz, 2H), 7.91 (d, J = 15.6 Hz, 1H), 7.76 (d, J = 7.0 Hz, 1H), 7.65 (t, J = 7.9 Hz, 1H), 7.46 (s, 1H), 7.28 (d, J = 8.3 Hz, 2H), 7.24 (s, 1H), 6.49 (d, J = 15.6 Hz, 1H), 6.27 (s, 2H). HRMS calcd for $C_{24}H_{15}N_3O_7$, 458.09894 $[M + H]^+$; found, 458.09772 $[M + H]^+$. Anal. ($C_{24}H_{15}N_3O_7$) C, H, N. MP > 260 °C.

(*E*)-4-(6-Isopropyl-2-(3-nitrostyryl)-4-oxoquinazolin-3(4*H*)-yl)-benzoic Acid (53). Compound **53** was prepared via procedure C using **53b** (0.150 g, 0.47 mmol) and *meta*-nitrobenzaldehyde (0.094 g, 0.62 mmol, 1.3 equiv) to yield the title compound as a yellow solid (0.137 g, 65%). ^{1}H NMR (400 MHz, DMSO-d_6) δ 13.34 (bs, 1H), 8.26 (d, 1H), 8.16 (d, J = 8.6 Hz, 2H), 8.00 (d, J = 15.7 Hz, 1H), 7.99 (d, J = 2.0 Hz, 1H), 7.87−7.83 (mult, 3H), 7.75 (d, J = 8.2 Hz, 1H), 7.66−7.61 (mult, 3H), 6.49 (d, J = 15.7 Hz, 1H), 3.11 (sept, J = 7.0 Hz, 1H), 1.29 (d, J = 7.0 Hz, 6H). ^{13}C NMR (100 MHz, DMSO-d_6) δ 166.8, 161.1, 149.9, 148.3, 147.6, 145.6, 140.7, 136.6, 136.3, 133.8, 133.3, 131.8, 130.7, 130.5, 129.4, 127.5, 123.9, 123.1, 122.7, 122.3, 120.4, 33.3, 23.7. HRMS calcd for $C_{26}H_{21}N_3O_5$, 456.15604 $[M + H]^+$; found, 456.15557 $[M + H]^+$. Anal. ($C_{26}H_{21}N_3O_5$) C, H, N. MP > 260 °C.

(*E*)-4-(2-(3-Nitrostyryl)-4-oxo-6-propylquinazolin-3(4*H*)-yl)-benzoic Acid (54). Compound **54** was prepared via procedure C using compound **54b** (0.578 g, 1.79 mmol) and *meta*-nitrobenzaldehyde (0.360 g, 2.38 mmol). The crude material was purified by silica gel chromatography (ISCO, RediSep 24 g column, silica cake, 0−10% MeOH/DCM gradient) to give a yellow solid (0.086 g, 11%). ^{1}H NMR (400 MHz, DMSO-d_6) δ 8.26 (s, 1H), 8.16 (d, J = 8.6 Hz, 3H), 7.96 (d, J = 15.6, 2H), 7.85 (d, J = 7.6 Hz, 1H), 7.79−7.73 (mult, 3H), 7.64 (t, J = 7.9 Hz, 3H), 6.50 (d,

J = 15.6 Hz, 1H), 2.75 (t, J = 7.3 Hz, 2H), 1.67 (sext, J = 7.3 Hz, 2H), 0.93 (t, J = 7.3 Hz, 3H). ^{13}C NMR (100 MHz, DMSO-d_6) δ 166.8, 161.1, 149.9, 148.3, 145.5, 141.5, 140.8, 136.6, 136.3, 135.7, 133.3, 131.6, 130.7, 130.5, 129.5, 127.3, 125.4, 123.9, 122.8, 122.3, 120.4, 36.8, 24.1, 13.5. HRMS calcd for $C_{26}H_{21}N_3O_5$, 456.15604 $[M + H]^+$; found, 456.15568 $[M + H]^+$. Anal. ($C_{26}H_{21}N_3O_5$) C, H, N. MP > 260 °C.

(*E*)-4-(2-(3-Nitrostyryl)-4-oxo-6-(thiophen-2-yl)quinazolin-3(4*H*)-yl)benzoic Acid (55). Compound **55a** (0.077 g, 0.212 mmol) was dissolved in a mixture of acetic acid (0.71 mL, 12.3 mmol, 58 equiv) and acetic anhydride (0.14 mL, 1.4 mmol, 7.0 equiv). To this solution was added *meta*-nitrobenzaldehyde (0.043 g, 0.283 mmol, 1.33 equiv) and sodium acetate (0.028 g, 0.35 mmol, 1.63 equiv). The mixture was refluxed for 6 h. After cooling to room temperature, the resultant yellow solid was collected by filtration and washed with methanol. The crude material was purified using silica gel chromatography (silica cake, ISCO, RediSep 24 g column, 0−10% MeOH/DCM gradient) to give a yellow solid (0.049 g, 48%). ^{1}H NMR (400 MHz, DMSO-d_6) δ 13.35 (bs, 1H), 8.31−8.25 (mult, 3H), 8.17 (d, J = 8.2 Hz, 3H), 8.03 (d, J = 15.7 Hz, 1H), 7.87 (t, J = 7.4 Hz, 2H), 7.74 (dd, J_1 = 3.5 Hz, J_2 = 1.2 Hz, 1H), 7.68−7.63 (mult, 4H), 7.21 (dd, J_1 = 5.1 Hz, J_2 = 3.51 Hz, 1H), 6.51 (d, J = 15.7 Hz, 1H). ^{13}C NMR (150 MHz, DMSO-d_6) δ 166.7, 160.9, 150.5, 148.3, 146.4, 141.9, 140.6, 136.8, 136.5, 131.3, 132.3, 131.9, 131.7, 130.7, 130.5, 129.4, 129.0, 128.3,126.8, 124.9, 124.0, 122.6, 122.4, 121.9, 121.2. HRMS calcd for $C_{27}H_{17}N_3O_5S$, 496.09683 $[M + H]^+$; found, 496.10655 $[M + H]^+$. Anal. ($C_{27}H_{17}N_3O_5S$) C, H, N. MP > 260 °C.

4-(2-(3-Nitrostyryl)-4-oxo-6-styrylquinazolin-3(4*H*)-yl)benzoic Acid (56). Compound **56a** (0.219 g, 0.57 mmol) was dissolved in a mixture of acetic acid (1.9 mL, 33 mmol, 58 equiv) and acetic anhydride (0.38 mL, 4.0 mmol, 7.0 equiv). To this solution was added *meta*-nitrobenzaldehyde (0.115 g, 0.76 mmol, 1.33 equiv) and sodium acetate (0.077 g, 0.93 mmol, 1.63 equiv). The mixture was refluxed for 6 h. The mixture was cooled to room temperature, and the resulting yellow solid was collected by filtration and washed with methanol. The crude material was purified using silica gel chromatography (silica cake, ISCO, RediSep 24 g column, 0−10% MeOH/DCM gradient) to give a yellow solid (0.146 g, 50%). ^{1}H NMR (400 MHz, $CDCl_3$) δ 8.27 (s, 1H), 8.17 (d, J = 7.8 Hz, 1H), 8.11 (d, J = 8.2 Hz, 2H), 8.03 (d, J = 15.3 Hz, 1H), 7.97 (s, 1H), 7.85−7.82 (mult, 2H), 7.65 (t, J = 8.2 Hz, 2H), 7.52 (d, J = 8.6 Hz, 2H), 7.44−7.24 (mult, 3H), 7.37−7.35 (mult, 2H), 6.52 (d, J = 15.6 Hz, 1H). HRMS calcd for $C_{31}H_{21}N_3O_5$, 516.15606 $[M + H]^+$; found, 516.14182 $[M + H]^+$. Anal. ($C_{31}H_{21}N_3O_5$) C, H, N. MP > 260 °C

(*E*)-4-(6-Methoxy-2-(3-nitrostyryl)-4-oxoquinazolin-3(4*H*)-yl)benzonitrile (58). Compound **58** was prepared via procedure C using compound **58a** (0.150 g, 0.520 mmol) and *meta*-nitrobenzaldehyde (0.103 g, 0.690 mmol, 1.33 equiv). The crude material was purified by recrystallization with hexanes and chloroform to yield the title compound as a bright-yellow solid (0.112 g, 51%). ^{1}H NMR (400 MHz, $CDCl_3$) δ 8.19−8.17 (mult, 2H), 8.00 (d, J = 15.7 Hz, 1H), 7.93 (d, J = 8.6 Hz, 2H), 7.76 (d, J = 9.0 Hz, 1H), 7.66 (d, J = 2.7 Hz, 1H), 7.63−7.61 (mult, 1H), 7.54 (d, J = 8.6 Hz, 1H), 7.51 (d, J = 8.6 Hz, 2H), 7.45 (dd, J_1 = 9.0 Hz, 1H), 3.95 (s, 3H). ^{13}C NMR (400 MHz, $CDCl_3$) δ 161.8, 159.3, 148.9, 147.2, 142.1, 141.2, 137.3, 137.0, 134.1, 132.9, 130.3, 130.1, 129.6, 125.7, 124.3, 122.8, 122.1, 121.8, 118.0, 114.0, 106.9, 56.1. HRMS calcd for $C_{24}H_{16}N_4O_4$, 425.12514 $[M + H]^+$; found, 425.12473 $[M + H]^+$. Anal. ($C_{24}H_{16}N_4O_4$) C, H, N. MP > 260 °C

(*E*)-4-(6-Methoxy-2-(3-nitrostyryl)-4-oxoquinazolin-3(4*H*)-yl)benzamide (59). Compound **59** was prepared via procedure C using compound **59a** (0.200 g, 0.650 mmol) and *meta*-nitrobenzaldehyde (0.130 g, 0.860 mmol, 1.33 equiv). The crude material was purified by hot gravity filtration after boiling with methanol and collection of the title compound as the resulting yellow solid (0.162 g, 57%). ^{1}H NMR (400 MHz, DMSO-d_6) δ 8.24 (s, 1H), 8.16 (d, J = 8.6 Hz, 2H), 8.09 (d, J = 8.6 Hz, 2H), 7.94 (d, J = 15.7 Hz, 1H), 7.83 (d, J = 7.8 Hz, 1H), 7.77 (d, J = 9.8 Hz, 1H), 7.64 (t, J = 7.8 Hz, 1H), 7.58 (d, J = 8.6 Hz, 2H), 7.54−7.51 (mult, 3H), 6.49 (d, J = 15.7 Hz, 1H), 3.91 (s, 3H). ^{13}C NMR (100 MHz,, DMSO-d_6) δ 167.1, 160.9, 158.1, 148.6, 148.3, 141.7, 139.4, 136.7, 135.7, 134.9, 133.1, 130.5, 129.2, 129.0, 128.9, 124.5, 123.8, 122.8, 122.2, 121.6, 55.8. HRMS calcd for $C_{24}H_{18}N_4O_5$, 443.13564; found, 443.13529 $[M + H]^+$. Anal. ($C_{24}H_{18}N_4O_5$) C, H, N. MP > 260 °C.

(*E*)-Methyl 4-(6-Methoxy-2-(3-nitrostyryl)-4-oxoquinazolin-3(4*H*)-yl)benzoate (60). Compound **60** was prepared via procedure C using compound **60a** (0.200 g, 0.650 mmol) and *meta*-nitrobenzaldehyde (0.124 g, 0.860 mmol, 1.33 equiv) to yield the title compound as a yellow solid (0.143 g, 51%). ^{1}H NMR (400 MHz, DMSO-d_6) δ 8.29 (d, J = 8.2 Hz, 2H), 8.15 (d, J = 6.7 Hz, 2H), 7.96 (d, J = 15.7 Hz, 1H), 7.76 (d, J = 9.0 Hz, 1H), 7.67 (d, J = 2.7 Hz, 1H), 7.59 (d, J = 7.8 Hz, 1H), 7.50 (t, J = 7.8 Hz, 1H), 7.45−7.43 (mult, 3H), 6.42 (d, J = 15.7 Hz, 1H), 4.01 (s, 3H), 3.95 (s, 3H). ^{13}C NMR (100 MHz, DMSO-d_6) δ 166.3, 161.9, 159.1, 148.8, 148.3, 142.2, 141.1, 137.2, 136.8, 132.9, 131.6, 131.5, 130.0, 129.5, 129.2, 125.5, 124.1, 122.7, 122.6, 121.9, 106.8, 56.4, 53.1. HRMS calcd for $C_{25}H_{19}N_3O_6$, 458.13534 $[M + H]^+$; found, 458.13473 $[M + H]^+$. Anal. ($C_{25}H_{19}N_3O_6$) C, H, N. MP > 260 °C.

(*E*)-4-(6-Methoxy-2-(3-methoxystyryl)-4-oxoquinazolin-3(4*H*)-yl)benzoic Acid (61). Compound **61** was prepared via procedure C using compound **46b** (0.200 g, 0.650 mmol) and *meta*-anisaldehyde (0.104 mL, 0.860 mmol, 1.33 equiv) to yield the title compound as a yellow solid (0.150 g, 54%). ^{1}H NMR (300 MHz, DMSO-d_6) δ 13.32 (bs, 1H), 8.16 (d, J = 8.5 Hz, 2H), 7.78 (d, J = 15.2 Hz, 1H), 7.75 (d, J = 9.4 Hz, 1H), 7.52−7.49 (mult, 2H), 7.26 (t, J = 7.9 Hz, 1H), 6.92 (d, J = 8.5 Hz, 3H), 6.28 (d, J = 15.5 Hz, 1H), 3.90 (s, 3H), 3.72 (s, 3H). ^{13}C NMR (100 MHz, DMSO-d_6) δ 166.7, 160.9, 159.5 157.7, 148.8, 141.9, 141.0, 138.0, 136.3, 131.6, 130.6, 130.1, 129.5, 129.0, 124.5, 121.3, 120.2, 119.1, 115.1, 113.5, 106.5, 55.7, 55.1. HRMS calcd for $C_{25}H_{20}N_2O_5$, 429.14514 $[M + H]^+$; found, 429.14404 $[M + H]^+$. Anal. ($C_{25}H_{20}N_2O_5$) C, H, N. MP > 260 °C.

(*E*)-3-(2-(3-(4-Carboxyphenyl)-6-methoxy-4-oxo-3,4-dihydroquinazolin-2-yl)vinyl)benzoic Acid (62). Compound **62** was prepared via procedure C using compound **46b** (0.200 g, 0.650 mmol) and *meta*-formylbenzoic acid (0.129 g, 0.860 mmol, 1.33 equiv) to yield the title compound as a yellow solid (0.259 g, 45%). ^{1}H NMR (400 MHz, DMSO-d_6) δ 8.16 (d, J = 8.6 Hz, 2H), 7.89 (mult, 3H), 7.76 (d, J = 9.5 Hz, 1H), 7.63 (d, J = 8.6 Hz, 2H), 7.53−7.50 (mult, 2H), 7.58 (t, J = 7.9 Hz, 1H), 6.37 (d, J = 15.6 Hz, 1H), 3.90 (s, 3H). ^{13}C NMR (100 MHz, DMSO-d_6) δ 166.8, 166.7, 160.9, 158.1, 148.7, 141.8, 141.0, 137.2, 135.3, 131.52, 131.49, 130.7, 130.2, 129.5, 129.1, 128.1, 124.5, 121.4, 120.9, 106.5, 55.8. HRMS calcd for $C_{25}H_{18}N_2O_6$, 443.12444 $[M + H]^+$; found, 443.12393 $[M + H]^+$. Anal. ($C_{25}H_{18}N_2O_6$) C, H, N. MP > 260 °C.

(*E*)-4-(6,7-Dimethoxy-2-(3-nitrostyryl)-4-oxoquinazolin-3(4*H*)-yl)benzoic Acid (63). Compound **63** was prepared via procedure C using compound **63b** (0.200 g, 0.59 mmol) and *meta*-nitrobenzaldehyde (0.118 g, 0.780 mmol, 1.33 equiv). The crude material was purified by hot gravity filtration after boiling with methanol to yield the title compound as a yellow solid (0.165 g, 59%). ^{1}H NMR (400 MHz, DMSO-d_6) δ 13.31 (bs, 1H), 8.18−8.14 (mult, 4H), 7.94 (d, J = 15.2 Hz, 1H), 7.81 (d, J = 7.8 Hz, 1H), 7.64−7.60 (mult, 3H), 7.42 (s, 1H), 7.26 (s, 1H), 6.45 (d, J = 15.2 Hz, 1H), 3.97 (s, 3H), 3.88 (s, 3H). ^{13}C NMR (100 MHz, DMSO-d_6) δ 172.1, 167.3, 160.3, 155.0, 149.4, 149.0, 148.3, 143.3, 136.7, 135.6, 133.0, 130.5, 130.3, 123.8, 122.9, 122.1, 114.2, 107.8, 105.8, 56.1, 55.8. HRMS calcd for $C_{25}H_{19}N_3O_7$, 474.13024 $[M + H]^+$; found, 474.13077 $[M + H]^+$. Anal. ($C_{25}H_{19}N_3O_7 \cdot 0.25H_2O$) C, H, N. MP > 260 °C.

(*E*)-4-(2-(3,4-Diacetoxystyryl)-6-methoxy-4-oxoquinazolin-3(4*H*)-yl)benzoic Acid (64). Compound **64** was prepared via procedure C using **46b** (0.400 g, 1.29 mmol) and 3,4-dihydroxybenzaldehyde (0.237 g, 1.71 g, 1.33 equiv). The crude material was purified by silica gel chromatography (ISCO, RediSep 40 g column, silica cake, 0−10% MeOH/DCM gradient) to yield the title compound as a yellow solid (0.221 g, 33%). ^{1}H NMR (400 MHz, DMSO-d_6) δ 8.15 (d, J = 8.3 Hz, 2H), 7.91 (d, J = 15.6 Hz, 1H),

7.76 (d, J = 7.6 Hz, 1H), 7.60 (d, J = 8.3 Hz, 2H), 7.52 (d, J = 7.3 Hz, 2H), 7.25 (d, J = 8.3 Hz, 1H), 6.32 (d, J = 15.6 Hz, 1H), 3.90 (s, 3H), 2.27 (s, 6H). ^{13}C NMR (100 MHz, DMSO-d_6) δ 168.81, 168.76, 161.5, 158.6, 149.4, 143.3, 143.0, 142.5, 141.5, 137.2, 134.4, 132.3, 131.3, 130.0, 129.8, 126.3, 125.1, 124.9, 123.4, 123.3, 122.0, 121.6, 107.2, 56.4, 21.02, 20.98. HRMS calcd for $C_{28}H_{22}N_2O_8$, 515.1510 $[M]^+$; found, 515.14526 $[M]^+$. Anal. ($C_{28}H_{22}N_2O_8$) C, H, N. MP 247−252 °C.

(*E*)-4-(6-Iodo-2-(4-nitrostyryl)-4-oxoquinazolin-3(4H)-yl)benzoic acid (72). Compound **72** was prepared via procedure C using compound **72b** (0.200 g, 0.490 mmol) and *para*-nitrobenzaldehyde (0.099 g, 0.65 mmol, 1.3 equiv) to yield the title compound as a yellow solid (0.174 g, 66%). ^{1}H NMR (400 MHz, DMSO-d_6) δ 8.32 (s, 1H), 8.16−8.12 (mult, 4H), 8.05 (s, 1H), 7.98 (d, J = 15.6 Hz, 1H), 7.77−7.68 (mult, 3H), 7.61−7.54 (mult, 2H), 6.41 (d, J = 15.6 Hz, 1H). ^{13}C NMR (150 MHz, DMSO-d_6) δ 166.6, 159.9, 151.4, 148.2, 146.4, 143.1, 137.0, 136.5, 136.4, 134.6, 133.3, 130.5, 130.1, 129.8, 129.3, 124.0, 122.5, 122.4, 122.1, 91.9. HRMS calcd for $C_{23}H_{14}IN_3O_5$, 540.00574 $[M + H]^+$; found, 540.00559 $[M + H]^+$. Anal. ($C_{23}H_{14}IN_3O_5$) C, H, N. MP > 260 °C.

(*E*)-3-(6-Iodo-2-(4-nitrostyryl)-4-oxoquinazolin-3(4*H*)-yl)benzoic Acid (73). Compound **73** was prepared via procedure C using compound **73b** (0.800 g, 1.97 mmol) and *para*-nitrobenzaldehyde (0.396 g, 2.62 mmol, 1.33 equiv) to yield the title compound as a yellow solid (0.572 g, 54%). ^{1}H NMR (400 MHz, DMSO-d_6) δ 13.29 (bs, 1H), 8.32 (mult, 1H), 8.16−8.09 (mult, 5H), 7.94 (d, J = 15.3 Hz, 1H), 7.77 (s, 2H), 7.65−7.54 (mult, 3H), 6.47 (d, J = 15.3 Hz, 1H). ^{13}C NMR (150 MHz, DMSO-d_6) δ 166.8, 158.7, 151.6, 148.7, 147.2, 142.8, 136.7, 136.6, 135.9, 134.3, 133.2, 130.8, 130.6, 129.4, 128.9, 128.8, 123.9, 123.5, 123.4, 122.1, 92.2. HRMS calcd for $C_{23}H_{14}IN_3O_5$, 540.00574 $[M + H]^+$; found, 540.00548 $[M + H]^+$. Anal. ($C_{23}H_{14}IN_3O_5$) C, H, N. MP > 260 °C.

(*E*)-3-(6-Iodo-2-(3-nitrostyryl)-4-oxoquinazolin-3(4*H*)-yl)benzoic Acid (74). Compound **74** was prepared via procedure C using compound **73b** (0.800 g, 1.97 mmol) and *meta*-nitrobenzaldehyde (0.396 g, 2.62 mmol, 1.33 equiv) to yield the title compound as a yellow solid (0.626 g, 59%). ^{1}H NMR (400 MHz, DMSO-d_6) δ 8.32 (s, 1H), 8.16−8.12 (mult, 4H), 8.05 (s, 1H), 7.98 (d, J = 15.6 Hz, 1H), 7.77−7.68 (mult, 3H), 7.61−7.54 (mult, 2H), 6.41 (d, J = 15.6 Hz, 1H). ^{13}C NMR (150 MHz, DMSO-d_6) δ 166.6, 159.9, 151.4, 148.2, 146.4, 143.1, 137.0, 136.5, 136.4, 134.6, 133.3, 130.5, 130.1, 129.8, 129.3, 124.0, 122.5, 122.4, 122.1, 91.9. HRMS calcd for $C_{23}H_{14}IN_3O_5$, 540.00574 $[M + H]^+$; found, 540.00546 $[M + H]^+$. Anal. ($C_{23}H_{14}IN_3O_5$), C, H, N. MP > 260 °C.

(*E*)-4-(6-Methoxy-2-(4-nitrostyryl)-4-oxoquinazolin-3(4*H*)-yl)-benzoic Acid (75). Compound **75** was prepared via procedure C using compound **46b** (0.730 g, 2.35 mmol) and *para*-nitrobenzaldehyde (0.473 g, 3.13 mmol, 1.3 equiv) to yield the title compound as a yellow solid (0.559 g, 54%). ^{1}H NMR (400 MHz, DMSO-d_6) δ 13.32 (bs, 1H), 8.17 (t, J = 8.8 Hz, 4H), 7.92 (d, J = 15.3, 1H), 7.78 (dd, J_1 = 10 Hz, J_2 = 4 Hz, 1H), 7.68 (d, J = 8.9 Hz, 1H), 7.63 (d, J = 8.2 Hz, 1H) 7.58−7.52 (mult, 2H), 6.51 (d, J = 15.7 Hz, 1H), 3.90 (s, 3H). ^{13}C NMR (100 MHz, DMSO-d_6) δ 166.7, 158.4, 148.3, 147.4, 141.7, 141.3, 140.7, 135.7, 130.7, 129.4, 128.6, 124.5, 124.2, 106.6, 55.8. HRMS calcd for $C_{24}H_{17}N_2O_6$, 444.11964 $[M + H]^+$; found, 444.11978 $[M + H]^+$. Anal. ($C_{24}H_{17}N_2O_6$) C, H, N. MP > 260 °C.

(*E*)-3-(6-Methoxy-2-(4-nitrostyryl)-4-oxoquinazolin-3(4*H*)-yl)-benzoic Acid (76). Compound **76** was prepared via procedure C using compound **76a** (0.730 g, 2.35 mmol) and *para*-nitrobenzaldehyde (0.473 g, 3.13 mmol, 1.3 equiv) to yield the title compound as a yellow solid (0.728 g, 70%). ^{1}H NMR (400 MHz, DMSO-d_6) δ 13.34 (bs, 1H), 8.13−8.18 (mult, 3H), 8.04 (s, 1H), 7.91 (d, J = 15.7 Hz, 1H), 7.74−7.79 (mult, 3H), 7.65 (d, J = 9.0 Hz, 2H), 7.51−7.54 (mult, 2H), 6.50 (d, J = 15.7 Hz, 1H), 3.90 (s, 3H). ^{13}C NMR (100 MHz, DMSO-d_6) δ 166.5, 161, 158.2, 148.6, 147.4, 141.7, 141.4, 137.1, 135.5, 133.4, 132.5, 130.1, 130, 129.2, 128.5, 124.4, 124.2, 124.2, 121.7, 106.6, 55.8. HRMS calcd for $C_{24}H_{17}N_3O_6$, 444.11964 $[M + H]^+$; found, 444.11978 $[M + H]^+$. Anal. ($C_{24}H_{17}N_2O_6$) C, H, N. MP > 260 °C.

(*E*)-3-(6-Methoxy-2-(3-nitrostyryl)-4-oxoquinazolin-3(4*H*)-yl)-benzoic Acid (77). Compound **77** was prepared via procedure C using compound **76a** (0.194 g, 0.626 mmol) and *meta*-nitrobenzaldehyde (0.126 g, 0.833 mmol, 1.3 equiv) to yield the title compound as a yellow solid (0.087 g, 33%). ^{1}H NMR (400 MHz, DMSO-d_6) δ 13.32 (bs, 1H), 8.21 (s, 1H), 8.13−8.15 (mult, 2H), 8.03 (s, 1H), 7.92 (d, J = 15.7 Hz, 1H), 7.82 (d, J = 7.8 Hz, 1H), 7.73−7.77 (mult, 3H), 7.61 (t, J = 8.0 Hz, 1H), 7.51−7.53 (mult, 2H), 6.47 (d, J = 15.7 Hz, 1H), 3.89 (s, 3H). (100 MHz, DMSO-d_6) δ 166.6, 161.0, 158.1, 148.7, 148.3, 141.7, 137.2, 136.8, 135.7, 133.5, 133.2, 132.4, 130.5, 130.1, 130, 129.2, 124.4, 123.8, 122.9, 122.1, 121.6, 106.6, 55.8. HRMS calcd for $C_{24}H_{17}N_3O_6$, 444.11964 $[M + H]^+$; found, 444.11957 $[M + H]^+$. Anal. ($C_{24}H_{17}N_2O_6$) C, H, N. MP > 260 °C.

4-(6-Iodo-2-methyl-4-oxoquinazolin-3(4*H*)-yl)benzoic Acid (78). Compound **78** was prepared via procedure B using compound **78a** (2.00 g, 7.00 mmol) and *para*-aminobenzoic acid (1.15 g, 8.40 mmol, 1.20 equiv). The crude material was recrystallized with ethyl acetate and methanol to give an off-white solid (1.27 g, 45%). ^{1}H NMR (400 MHz, DMSO-d_6) δ 13.27 (bs, 1H), 8.36 (d, J = 2.0 Hz, 1H), 8.15−8.11 (mult, 3H), 7.61 (d, J = 8.5 Hz, 2H), 7.47 (d, J = 8.5 Hz, 1H), 2.11 (s, 3H). ^{13}C NMR (100 MHz, DMSO-d_6) δ166.7, 160.0, 1547, 146.6, 143.0, 141.5, 134.5, 131.5, 130.7, 128.9, 122.3, 91.3, 24.2. HRMS calcd for $C_{16}H_{11}IN_2O_3$, 406.98934 $[M + H]^+$; found, 406.98893 $[M + H]^+$.

(*E*)-4-(6-Iodo-4-oxo-2-styrylquinazolin-3(4*H*)-yl)benzoic Acid (79). Compound **79** was prepared via procedure C using compound **45b** (0.300 g, 0.740 mol) and benzaldehyde (0.100 mL, 0.980 mmol, 1.33 equiv). The crude material was purified by hot gravity filtration of the title compound as a yellow solid after boiling in methanol (0.070 g, 19%). ^{1}H NMR (400 MHz, DMSO-d_6) δ 8.40 (d, J = 1.9 Hz, 1H), 8.19−8.15 (mult, 3H), 7.92 (d, J = 15.5 Hz, 1H), 7.62−7.57 (mult, 3H), 7.39−7.35 (mult, 5H), 6.30 (d, J = 15.5 Hz, 1H). ^{13}C NMR (150 MHz, DMSO-d_6) δ 166.8, 160.0, 151.6, 146.7, 143.2, 140.4, 139.7, 134.6, 132.3, 130.7, 130.0,129.3, 129.2, 129.0, 127.7, 122.4, 119.5, 114.0, 91.5. HRMS calcd for $C_{23}H_{15}IN_2O_3$, 495.02064; found, 495.01987 $[M + H]^+$. Anal. ($C_{23}H_{15}IN_2O_3$) C, H, N. MP > 260 °C.

4-(6-Methyl-4-oxo-2-phenethylquinazolin-3(4*H*)-yl)benzoic Acid (81). Compound **80** (0.100 g, 0.26 mmol) was dissolved in DMF (5.0 mL). Palladium on carbon (10%, 0.10 g, 10 wt %) was added. A balloon filled with hydrogen was added, and the mixture was stirred at room temperature for 1 h. The mixture was filtered over a pad of Celite, and the resulting solution was concentrated in vacuo to give a white solid. The solid was triturated with DCM and obtained by filtration (0.016 g, 16%). ^{1}H NMR (400 MHz, DMSO-d_6) δ 13.27 (bs, 1H), 8.09 (d, J = 8.2 Hz, 2H), 7.93 (s, 1H), 7.71 (d, J = 8.6 Hz, 1H), 7.65 (d, J = 8.2 Hz, 1H), 7.54 (d, J = 8.1 Hz, 2H), 7.22 (t, J = 7.4 Hz, 2H), 7.14 (t, J = 7.0 Hz, 1H), 7.06 (d, J = 7.0 Hz, 2H), 2.98 (t, J = 7.4 Hz, 2H), 2.58 (t, J = 7.4 Hz, 2H), 2.47 (s, 3H). ^{13}C NMR (100 MHz, DMSO-d_6) δ 166.7, 161.2, 154.6, 145.1, 141.3, 140.8, 136.4, 136.1, 131.5, 130.5, 129.2, 128.4, 128.2, 126.9, 126.1, 125.7, 120.2, 37.1, 32.0, 20.8. HRMS calcd for $C_{24}H_{20}N_2O_3$, 385.15534 $[M + H]^+$; found, 385.15459 $[M + H]^+$. Anal. ($C_{24}H_{20}N_2O_3$) C: 72.02, H: 5.03, N: 7.19. MP > 260 °C

(*E*)-4-(6-Iodo-4-oxo-2-(2-(pyridin-3-yl)vinyl)quinazolin-3(4*H*)-yl)benzoic Acid (98). Compound **98** was prepared via procedure C using compound **72b** (0.240 g, 0.591 mmol) and nicotinaldehyde (0.084 g, 0.074 mL, 0.786 mmol, 1.33 equiv). The reaction mixture was filtered and washed with MeOH to give the title compound as a yellow solid (0.170 g, 58%). ^{1}H NMR (400 MHz, DMSO-d_6) δ 13.31 (bs, 1H), 8.67 (d, J = 2.4 Hz, 1H), 8.52 (dd, J_1 = 4.7 Hz, J_2 = 1.6 Hz, 1H), 8.41 (d, J = 2.0 Hz, 1H), 8.19 (dd, J_1 = 8.4 Hz, J_2 = 8.4 Hz, 1H), 8.15 (d, J = 8.6 Hz, 2H), 7.93 (d, J = 15.7 Hz, 1H), 7.79 (d, J = 8.2 Hz, 1H), 7.58−7.63 (mult, 3H), 7.37 (dd, J_1 = 8.0 Hz, J_2 = 4.9 Hz, 1H), 6.43 (d, J = 15.7 Hz, 1H). ^{13}C NMR (100 MHz, DMSO-d_6) δ 166.7, 159.9, 151.3, 149.5, 146.6, 143.3, 140.5, 136.3, 133.9, 131.7, 130.7, 130.5, 129.3, 124.1, 122.5, 121.6, 91.9. HRMS calcd for $C_{22}H_{14}IN_3O_3$,494.00006 $[M - H]^+$; found, 494.00150 $[M - H]^+$. Anal. ($C_{22}H_{14}IN_3O_3$) C, H, N. MP > 260 °C.

(*E*)-3-(6-Iodo-4-oxo-2-(2-(pyridin-3-yl)vinyl)quinazolin-3(4*H*)-yl)-benzoic Acid (99). Compound **99** was prepared via procedure C using compound **73b** (0.300 g, 0.739 mmol) and nicotinaldehyde (0.105 g, 0.092 mL, 0.982 mmol, 1.3 equiv) The reaction mixture was recrystallized from ethyl acetate and hexanes to give the title compound as a yellow solid (0.111 g, 30%). ^{1}H NMR (400 MHz, DMSO-d_6) δ 13.31 (bs, 1H), 8.65 (s, 1H), 8.51 (d, J = 3.9 Hz, 1H), 8.39 (s, 1H), 8.16 (t, J = 9.4 Hz, 2H), 8.05 (s, 1H), 7.92 (d, J = 15.7 Hz, 1H), 7.74−7.78 (mult, 3H), 7.58 (d, J = 8.6 Hz, 1H), 7.34−7.37 (mult, 1H), 6.42 (d, J = 15.7 Hz, 1H). ^{13}C NMR (100 MHz, DMSO-d_6) δ 166.5, 160.1, 151.6, 150.5, 149.5, 146.6, 143.2, 136.9, 136.1, 134.7, 133.9, 133.4, 132.4, 130.5, 130.2, 130.1, 129.9, 129.4, 124.1, 122.6, 121.7, 91.8. HRMS calcd for $C_{22}H_{14}IN_3O_3$ 494.00006 $[M - H]^+$; found, 494.00165 $[M - H]^+$. Anal. ($C_{22}H_{14}IN_3O_3$) C: 45.18, H: 2.23, N: 7.16. MP > 260 °C.

Acknowledgment. We thank Serdar Kurtkaya for helpful discussions. This work was supported by the Michael J. Fox Foundation (S.F.T.), the Alfred Benzon Foundation (K.B.H.), the Villum Kann Rasmussen Foundation (K.B.H.), the Lundbeck Foundation (K.B.H.), the Carlsberg Foundation (H.B.O.), the GluTarget Center of Excellence (H.B.O.), the NIH (NS065371, NS036654, S.F.T.), Pharmacological Sciences Training grant (T32 GM008602, T.M.A.), and a research grant from Pfizer (S.F.T.). The authors declare no competing financial interests.

Supporting Information Available: Experimental information, representative current recording from a *Xenopus* oocyte expressing NR1/NR2D in response to 100 μM glutamate/30 μM glycine plus increasing concentrations of compound **2**; composite concentration−effect curves for compound **2**, representative current recording showing that inhibition by compound **2** cannot be surmounted by increasing concentrations of agonist, current−voltage relationship for responses to glutamate plus glycine (100 μM and 30 μM, respectively) in the absence and presence of 10 μM compound **2**, current−voltage relationship for responses to glutamate plus glycine (100 μM and 30 μM, respectively) in the absence and presence of 10 μM compound **2**; general formula for experimental test compounds described in Tables 1−7; plot of IC_{50} values determined by two-electrode voltage-clamp recordings from *Xenopus* oocytes versus the side chain van der Waals radii, plot of selectivity. This material is available free of charge via the Internet at http://pubs.acs.org.

References

(1) Traynelis, S. F.; Wollmuth, L. P.; McBain, C. J.; Menniti, F. S.; Vance, K. M.; Ogden, K. K.; Hansen, K. B.; Yuan,H.; Myers, S. J.; Dingledine, R. Glutamate receptor ion channels: structure, regulation, and function, *Pharmacol. Rev.* **2010**, *62*, manuscript in press, DOI 10.1124/pr.109.002451.

(2) Rudhard, Y.; Kneussel, M.; Nassar, M. A.; Rast, G. F.; Annala, A. J.; Chen, P. E.; Tigaret, C. M.; Dean, I.; Roes, J.; Gibb, A. J.; Hunt, S. P.; Schoepfer, R. Absence of Whisker-related pattern formation in mice with NMDA receptors lacking coincidence detection properties and calcium signaling. *J. Neurosci.* **2003**, *23*, 2323–2332.

(3) Colonnese, M. T.; Shi, J.; Constantine-Paton, M. Chronic NMDA receptor blockade from birth delays the maturation of NMDA currents, but does not affect AMPA/kainate currents. *J. Neurophysiol.* **2003**, *89*, 57–68.

(4) Waters, K. A.; Machaalani, R. Role of NMDA receptors in development of respiratory control. *Respir. Physiol. Neurobiol.* **2005**, *149*, 123–130.

(5) Nacher, J.; McEwen, B. S. The role of *N*-methyl-D-asparate receptors in neurogenesis. *Hippocampus* **2006**, *16*, 267–270.

(6) Lisman, J. Long-term potentiation: outstanding questions and attempted synthesis. *Philos. Trans. R. Soc., B* **2003**, *358*, 829–842.

(7) Miyamoto, E. Molecular mechanism of neuronal plasticity: induction and maintenance of long-term potentiation in the hippocampus. *J. Pharmacol. Sci.* **2006**, *100*, 433–442.

(8) Walsh, T.; McClellan, J. M.; McCarthy, S. E.; Addington, A. M.; Pierce, S. B.; Cooper, G. M.; Nord, A. S.; Kusenda, M.; Malhotra, D.; Bhandari, A.; Stray, S. M.; Rippey, C. F.; Roccanova, P.; Makarov, V.; Lakshmi, B.; Findling, R. L.; Sikich, L.; Stromberg, T.; Merriman, B.; Gogtay, N.; Butler, P.; Eckstrand, K.; Noory, L.; Gochman, P.; Long, R.; Chen, Z.; Davis, S.; Baker, C.; Eichler, E. E.; Meltzer, P. S.; Nelson, S. F.; Singleton, A. B.; Lee, M. K.; Rapoport, J. L.; King, M. C.; Sebat, J. Rare structural variants disrupt multiple genes in neurodevelopmental pathways in schizophrenia. *Science* **2008**, *320*, 539–543.

(9) Lindahl, J. S.; Keifer, J. Glutamate receptor subunits are altered in forebrain and cerebellum in rats chronically exposed to the NMDA receptor antagonist phencyclidine. *Neuropsychopharmacology* **2004**, *29*, 2065–2073.

(10) Whetsell, W. O., Jr. Current concepts of excitotoxicity. *J. Neuropathol. Exp. Neurol.* **1996**, *55*, 1–13.

(11) Dirnagl, U.; Iadecola, C.; Moskowitz, M. A. Pathobiology of ischaemic stroke: an integrated view. *Trends Neurosci.* **1999**, *22*, 391–397.

(12) Bräuner-Osborne, H.; Egebjerg, J.; Nielsen, E. O.; Madsen, U.; Krogsgaard-Larsen, P. Ligands for glutamate receptors: design and therapeutic prospects. *J. Med. Chem.* **2000**, *43*, 2609–2645.

(13) Wang, C. X.; Shuaib, A. NMDA/NR2B selective antagonists in the treatment of ischemic brain injury. *Curr. Drug Targets CNS Neurol. Disord.* **2005**, *4*, 143–151.

(14) Miyabe, M.; Kirsch, J. R.; Nishikawa, T.; Koehler, R. C.; Traystman, R. J. Comparative analysis of brain protection by *N*-methyl-D-aspartate receptor antagonists after transient focal ischemia in cats. *Crit. Care Med.* **1997**, *25*, 1037–1043.

(15) Preskorn, S. H. How multiple medication use evolves and the importance of therapeutic trials: the slippery slide. *J. Psychiatr. Pract.* **2008**, *14*, 170–175.

(16) Stern, P.; Behe, P.; Schoepfer, R.; Colquhoun, D. Single-channel conductances of NMDA receptors expressed from cloned cDNAs: comparison with native receptors. *Proc. Biol. Sci.* **1992**, *250*, 271–277.

(17) Erreger, K.; Chen, P. E.; Wyllie, D. J.; Traynelis, S. F. Glutamate receptor gating. *Crit. Rev. Neurobiol.* **2004**, *16*, 187–224.

(18) Erreger, K.; Dravid, S. M.; Banke, T. G.; Wyllie, D. J.; Traynelis, S. F. Subunit-specific gating controls rat NR1/NR2A and NR1/NR2B NMDA channel kinetics and synaptic signalling profiles. *J. Physiol.* **2005**, *563*, 345–358.

(19) Erreger, K.; Geballe, M. T.; Dravid, S. M.; Snyder, J. P.; Wyllie, D. J.; Traynelis, S. F. Mechanism of partial agonism at NMDA receptors for a conformationally restricted glutamate analog. *J. Neurosci.* **2005**, *25*, 7858–7866.

(20) Monyer, H.; Sprengel, R.; Schoepfer, R.; Herb, A.; Higuchi, M.; Lomeli, H.; Burnashev, N.; Sakmann, B.; Seeburg, P. H. Heteromeric NMDA receptors: molecular and functional distinction of subtypes. *Science* **1992**, *256*, 1217–1221.

(21) Wyllie, D. J.; Behe, P.; Colquhoun, D. Single-channel activations and concentration jumps: comparison of recombinant NR1a/NR2A and NR1a/NR2D NMDA receptors. *J. Physiol.* **1998**, *510*, 1–18.

(22) Vicini, S.; Wang, J. F.; Li, J. H.; Zhu, W. J.; Wang, Y. H.; Luo, J. H.; Wolfe, B. B.; Grayson, D. R. Functional and pharmacological differences between recombinant *N*-methyl-D-aspartate receptors. *J. Neurophysiol.* **1998**, *79*, 555–566.

(23) Monyer, H.; Burnashev, N.; Laurie, D. J.; Sakmann, B.; Seeburg, P. H. Developmental and regional expression in the rat brain and functional properties of four NMDA receptors. *Neuron* **1994**, *12*, 529–540.

(24) Akazawa, C.; Shigemoto, R.; Bessho, Y.; Nakanishi, S.; Mizuno, N. Differential expression of five *N*-methyl-D-aspartate receptor subunit mRNAs in the cerebellum of developing and adult rats. *J. Comp. Neurol.* **1994**, *347*, 150–160.

(25) Buller, A. L.; Larson, H. C.; Schneider, B. E.; Beaton, J. A.; Morrisett, R. A.; Monaghan, D. T. The molecular basis of NMDA receptor subtypes: native receptor diversity is predicted by subunit composition. *J. Neurosci.* **1994**, *14*, 5471–5484.

(26) Dunah, A. W.; Luo, J.; Wang, Y. H.; Yasuda, R. P.; Wolfe, B. B. Subunit composition of *N*-methyl-D-aspartate receptors in the central nervous system that contain the NR2D subunit. *Mol. Pharmacol.* **1998**, *53*, 429–437.

(27) Thompson, C. L.; Drewery, D. L.; Atkins, H. D.; Stephenson, F. A.; Chazot, P. L. Immunohistochemical localization of *N*-methyl-D-aspartate receptor subunits in the adult murine hippocampal formation: evidence for a unique role of the NR2D subunit. *Mol. Brain Res.* **2002**, *102*, 55–61.

(28) Lau, W. K.; Lui, P. W.; Wong, C. K.; Chan, Y. S.; Yung, K. K. Differential expression of *N*-methyl-D-aspartate receptor subunit messenger ribonucleic acids and immunoreactivity in the rat

neostriatum during postnatal development. *Neurochem. Int.* **2003**, *43*, 47–65.
(29) Lopez de Armentia, M.; Sah, P. Development and subunit composition of synaptic NMDA receptors in the amygdala: NR2B synapses in the adult central amygdala. *J. Neurosci.* **2003**, *23*, 6876–6883.
(30) Dunah, A. W.; Standaert, D. G. Subcellular segregation of distinct heteromeric NMDA glutamate receptors in the striatum. *J. Neurochem.* **2003**, *85*, 935–943.
(31) Dunah, A. W.; Yasuda, R. P.; Wang, Y. H.; Luo, J.; Davila-Garcia, M.; Gbadegesin, M.; Vicini, S.; Wolfe, B. B. Regional and ontogenic expression of the NMDA receptor subunit NR2D protein in rat brain using a subunit-specific antibody. *J. Neurochem.* **1996**, *67*, 2335–2345.
(32) Hallett, P. J.; Standaert, D. G. Rationale for and use of NMDA receptor antagonists in Parkinson's disease. *Pharmacol. Ther.* **2004**, *102*, 155–174.
(33) Salter, M. G.; Fern, R. NMDA receptors are expressed in developing oligodendrocyte processes and mediate injury. *Nature* **2005**, *438*, 1167–1171.
(34) Karadottir, R.; Cavelier, P.; Bergersen, L. H.; Attwell, D. NMDA receptors are expressed in oligodendrocytes and activated in ischaemia. *Nature* **2005**, *438*, 1162–1166.
(35) Karavanova, I.; Vasudevan, K.; Cheng, J.; Buonanno, A. Novel regional and developmental NMDA receptor expression patterns uncovered in NR2C subunit-beta-galactosidase knock-in mice. *Mol. Cell. Neurosci.* **2007**, *34*, 468–480.
(36) Paquet, M.; Tremblay, M.; Soghomonian, J. J.; Smith, Y. AMPA and NMDA glutamate receptor subunits in midbrain dopaminergic neurons in the squirrel monkey: an immunohistochemical and in situ hybridization study. *J. Neurosci.* **1997**, *17*, 1377–1396.
(37) Carter, C.; Benavides, J.; Legendre, P.; Vincent, J. D.; Noel, F.; Thuret, F.; Lloyd, K. G.; Arbilla, S.; Zivkovic, B.; Mackenzie, E. T.; Scatton, B.; Langer, S. Z. Ifenprodil and Sl-82.0715 as Cerebral Anti-Ischemic Agents 0.2. Evidence for *N*-Methyl-D-Aspartate Receptor Antagonist Properties. *J. Pharmacol. Exp. Ther.* **1988**, *247*, 1222–1232.
(38) Gotti, B.; Duverger, D.; Bertin, J.; Carter, C.; Dupont, R.; Frost, J.; Gaudilliere, B.; Mackenzie, E. T.; Rousseau, J.; Scatton, B.; Wick, A. Ifenprodil and Sl-82.0715 as Cerebral Anti-Ischemic Agents 0.1. Evidence for Efficacy in Models of Focal Cerebral-Ischemia. *J. Pharmacol. Exp. Ther.* **1988**, *247*, 1211–1221.
(39) Williams, K. Ifenprodil discriminates subtypes of the *N*-methyl-D-aspartate receptor: selectivity and mechanisms at recombinant heteromeric receptors. *Mol. Pharmacol.* **1993**, *44*, 851–859.
(40) Hess, S. D.; Daggett, L. P.; Deal, C.; Lu, C. C.; Johnson, E. C.; Velicelebi, G. Functional characterization of human *N*-methyl-D-aspartate subtype 1A/2D receptors. *J. Neurochem.* **1998**, *70*, 1269–1279.
(41) Feng, B.; Tse, H. W.; Skifter, D. A.; Morley, R.; Jane, D. E.; Monaghan, D. T. Structure−activity analysis of a novel NR2C/NR2D-preferring NMDA receptor antagonist: 1-(phenanthrene-2-carbonyl) piperazine-2,3-dicarboxylic acid. *Br. J. Pharmacol.* **2004**, *141*, 508–516.
(42) Morley, R. M.; Tse, H. W.; Feng, B.; Miller, J. C.; Monaghan, D. T.; Jane, D. E. Synthesis and pharmacology of N1-substituted piperazine-2,3-dicarboxylic acid derivatives acting as NMDA receptor antagonists. *J. Med. Chem.* **2005**, *48*, 2627–2637.
(43) Frizelle, P. A.; Chen, P. E.; Wyllie, D. J. Equilibrium constants for (*R*)-[(*S*)-1-(4-bromo-phenyl)-ethylamino]-(2,3-dioxo-1,2,3,4-tetrahydroquino xalin-5-yl)-methyl]-phosphonic acid (NVP-AAM077) acting at recombinant NR1/NR2A and NR1/NR2B *N*-methyl-D-aspartate receptors: implications for studies of synaptic transmission. *Mol. Pharmacol.* **2006**, *70*, 1022–1032.
(44) Neyton, J.; Paoletti, P. Relating NMDA receptor function to receptor subunit composition: limitations of the pharmacological approach. *J. Neurosci.* **2006**, *26*, 1331–1333.
(45) Brothwell, S. L.; Barber, J. L.; Monaghan, D. T.; Jane, D. E.; Gibb, A. J.; Jones, S. NR2B- and NR2D-containing synaptic NMDA receptors in developing rat substantia nigra pars compacta dopaminergic neurones. *J. Physiol.* **2008**, *586*, 739–750.
(46) Mayer, M. L.; Armstrong, N. Structure and function of glutamate receptor ion channels. *Annu. Rev. Physiol.* **2004**, *66*, 161–181.
(47) Chen, P. E.; Geballe, M. T.; Stansfeld, P. J.; Johnston, A. R.; Yuan, H.; Jacob, A. L.; Snyder, J. P.; Traynelis, S. F.; Wyllie, D. J. Structural features of the glutamate binding site in recombinant NR1/NR2A *N*-methyl-D-aspartate receptors determined by site-directed mutagenesis and molecular modeling. *Mol. Pharmacol.* **2005**, *67*, 1470–1484.
(48) Dravid, S. M.; Erreger, K.; Yuan, H.; Nicholson, K.; Le, P.; Lyuboslavsky, P.; Almonte, A.; Murray, E.; Mosely, C.; Barber, J.; French, A.; Balster, R.; Murray, T. F.; Traynelis, S. F. Subunit-specific mechanisms and proton sensitivity of NMDA receptor channel block. *J. Physiol.* **2007**, *581*, 107–128.
(49) Yuan, H.; Hansen, K. B.; Vance, K. M.; Ogden, K. K.; Traynelis, S. F. Control of *N*-methyl-D-aspartate Receptor Function by the NR2 Subunit Amino-Terminal Domain. *J. Neurosci.* **2009**, *29*, 12045–12058.
(50) Sobolevsky, A. I.; Koshelev, S. G.; Khodorov, B. I. Probing of NMDA channels with fast blockers. *J. Neurosci.* **1999**, *19*, 10611–10626.
(51) Furukawa, H.; Singh, S. K.; Mancusso, R.; Gouaux, E. Subunit arrangement and function in NMDA receptors. *Nature* **2005**, *438*, 185–192.
(52) Karakas, E.; Simorowski, N.; Furukawa, H. Structure of the zinc-bound amino-terminal domain of the NMDA receceptor NR2B subunit. *EMBO J.* **2009**, *28*, 3910–3920.
(53) Hansen, K. B.; Bräuner-Osborne, H.; Egebjeg, J. Pharmacological Characterization of Ligands at Recombinant NMDA Receptor Subtypes by Electrophysiological Recordings and Intracellular Calcium Measurements. *Comb. Chem. High Throughput Screening* **2009**, *11*, 304–315.
(54) Menniti, F. S.; Chenard, B. L.; Collins, M. B.; Ducat, M. F.; Elliott, M. L.; Ewing, F. E.; Huang, J. I.; Kelly, K. A.; Lazzaro, J. T.; Pagnozzi, M. J.; Weeks, J. L.; Welch, W. M.; White, W. F. Characterization of the binding site for a novel class of noncompetitive alpha-amino-3-hydroxy-5-methyl-4-isoxazolepropionic acid receptor antagonists. *Mol. Pharmacol.* **2000**, *58*, 1310–1317.
(55) Welch, W. M.; Ewing, F. E.; Huang, J.; Menniti, F. S.; Pagnozzi, M. J.; Kelly, K.; Seymour, P. A.; Guanowsky, V.; Guhan, S.; Guinn, M. R.; Critchett, D.; Lazzaro, J.; Ganong, A. H.; DeVries, K. M.; Staigers, T. L.; Chenard, B. L. Atropisomeric quinazolin-4-one derivatives are potent noncompetitive alpha-amino-3-hydroxy-5-methyl-4-isoxazolepropionic acid (AMPA) receptor antagonists. *Bioorg. Med. Chem. Lett.* **2001**, *11*, 177–181.
(56) Lazzaro, J. T.; Paternain, A. V.; Lerma, J.; Chenard, B. L.; Ewing, F. E.; Huang, J.; Welch, W. M.; Ganong, A. H.; Menniti, F. S. Functional characterization of CP-465,022, a selective, noncompetitive AMPA receptor antagonist. *Neuropharmacology* **2002**, *42*, 143–153.
(57) Perich, J. W.; Johns, R. B. An Improved One-Pot Synthesis of *N*-alpha-(*tert*-Butoxycarbonyl)-*O*-(*O*′,*O*″-dialkylphosphoro)-L-Tyrosines Using Dialkyl *N*,*N*-Diethylphosphoramidites. *Synthesis* **1989**, 701–703.
(58) Hansen, K. B.; Mullasseril, P.; Dawit, S.; Kurtkaya, N. L.; Yuan, H.; Vance, K. M.; Orr, A. G.; Kvist, T.; Ogden, K. K.; Le, P.; Vellano, K. M.; Lewis, I.; Kurtkaya, S.; Du, Y.; Qui, M.; Murphy, T. J.; Snyder, J. P.; Bräuner-Osborne, H.; Traynelis, S. F. *J. Pharmacol. Exp. Ther.* **2010**, *333*, 650–662.
(59) Traynelis, S. F.; Burgess, M. F.; Zheng, F.; Lyuboslavsky, P.; Powers, J. L. Control of voltage-independent zinc inhibition of NMDA receptors by the NR1 subunit. *J. Neurosci.* **1998**, *18*, 6163–6175.